Response to Reviewer 1

We are grateful to the reviewer for the very careful and thorough examination of our manuscript. We think the revised manuscript is substantially improved as a result.

Specific Comments:

1-1. Page 2, line 24: I do not understand the use of 'if' in this sentence.

1-2. Line 29: I would write 'versus' instead of '/' in 'RASS/radiosonde'.

Response:

1-1. We have revised the manuscript and eliminated the text beginning with "if" (line 24).

1-2. Done (line 28).

2-1. Page 3, line 47: 'measures' => I suggest 'provides'

2-2. Line 48: I would add 'from the measurement of the Doppler shift between the emitted and backscattered radar wave', after 'propagates vertically'

2-3. Line 49: 'among' => 'between'

Response:

2-1. Done (line 46).

2-2. We have added 'from the measurement of the Doppler spectrum" in lines 47–48 to make it consistent with the Doppler spectrum in Fig. 4.

2-3. Done (line 49).

3-1. Page 4, lines (54-55): This issue about the vertical velocity correction is very important and not well presented. It is obvious that w has to be included. The fact that you could not use w is an issue, and you show in the following how you cope with it (1-hour averages). The way the issue is introduced, at the beginning of the paper, is not satisfying especially the sentence : 'the vertical wind speed is considered in Eq (1) because the neglect of the wind velocity ....'. I explain why.

At the beginning (p 4), it is obvious that the correction has to be done. You mention p 7 (lines 112- 115), that w could not be used due to the automobiles echo. So I deduced you had used the oblique beams instead of the vertical one. I understood in the following that you did not. Please, could you clarify this issue in your presentation, perhaps by saying at the beginning that you had to neglect w and that this issue would have to be discussed?

3-2. If you cite May's and Angevine's papers it could be interesting to add (further on in the manuscript) some details of their discussion, including the discussion on the downward bias in the profiler velocity measurements mentioned in Angevine et al., 1998: the 1-hour average is a way to mitigate this effect.

Response:

3-1. We have added an explanation for this comment (lines 56–59 and 136–138): "However, we do not consider the radial wind speed in our experiments, because strong clutter sometimes contaminates the Doppler spectrum and masks the atmospheric echo in the vertical beam observation. This issue is addressed in later sections.", and "Indeed, the vertical velocity correction can decrease the accuracy of RASS in situations with calm wind and a lower reliability of vertical wind measurements (Görsdorf and Lehmann 2000)."

3-2. We have modified the manuscript to respond to this comment (lines 209–211): "Using the hourly mean may also reduce the daytime downward bias (e.g., Görsdorf and Lehmann 2000; Adachi et al., 2005), which could be attributable to insects or hydrometeors that are undetectable (Angevine, 1997)."

4-1. Line 63: I would add 'accurate' before 'corrections'

4-2. Line 64: if relevant, I would add 'thermodynamic' before 'constants'

Response:

4-1. Done (Line 82).

4-2. Done (Line 83).

5. Minor comment: in lines 57, 59 and 61 respectively, you use brackets for two different purposes: with 'bias (systematic error)', 'standard deviation (precision)', the brackets provide the meanings whereas in 'bias (standard deviation)', you present an alternative. The latter use of the brackets is continued through the manuscript. The first use could be presented in a different way.

Response: We have revised out text to respond to this comment (lines 60–62): "The systematic error or bias of the virtual temperature measurements", and "while the standard deviation or precision has also been reported around 1°C.".

6-1. Lines 61 to 64: I was not convinced by the results you cite (Görsdorf's and Lehman's work) as long as I had not read the paper. My reservation was about the one year time average that reduced the bias as expected. When reading this paper, I was convinced and I found additional interesting information that would deserve to be discussed in your own paper (but probably not in the introduction):

- the reason for the range correction would be helpful to comment (see my point, Page 16, line 245). Görsdorf and Lehman are not the only ones who mention this range correction: Angevine et al., 1998 also do, but in the references you cite, Görsdorf and Lehman discuss the benefit of the correction at the inversion levels, which is a major advance and could feed your discussion.

- the distinction between climatological investigation and individual profile comparison is also an important point to comment: you can hardly compare errors amounts when they are computed with

varying time-scales (unless you discuss the conditions).

To conclude, I would say that the use of this reference comes too early and that you could take more advantage in discussing it further on.

6.2. In general, I suggest that you give more details about the results and the uncertainties that are reported in the literature, concerning the RASS assessment. For instance, Angevine et al., 1998 made a comparison of Tv during 1 month, at one level (396m agl) between a RASS system (UHF) and tower instruments. The uncertainties that they reported are expected to be different from those obtained for instance by Moran and Strauch (1994) who used a RASS with a VHF profiler, during 5 weeks (400 profiles, compared to RS). Moreover, in each case, some information should be given about the corrections (vertical velocity correction, range correction ...).

Response:

6-1. We appreciate the reviewer's suggestion. However, we did not find any discussion on the benefit of the range correction at the inversion levels in Görsdorf and Lehmann (2000). Instead, we have added an explanation to respond to the comment (lines 387–388): "the discrepancies in and below the inversion could be mitigated by considering the effect of the vertical airflow and/or **applying a range correction** "

6-2. We have revised the manuscript to refer more details reported in the literature and respond this comment (line 62-83): "May et al. (1989) compared..."

7. Page 5, line 66: you could also add 'the distortion of the acoustic wave due to turbulence and vertical temperature gradients (Lataitis, 1992)'

   Response: We have revised the text to respond to the comment (lines 86–87): "…in addition to the effects of **turbulence and vertical temperature gradients** (Lataitis, 1992)."

8. Line 68 : 'A wind profiler/RASS has been used'=>Joined measurements of wind profiler and RASS have been frequently used'.

   Response: We have revised the text to respond to this comment (line 88): "A wind profiler with RASS has been frequently used"

9. Line 71: 'Important limitations of this method include the emission' => 'Among the limitations of this method, an important one is the emission'

   Response: Done (lines 91–92).

10. Line 80 : 'is expected' => 'would be promising'

   Response: We have replaced "is expected" with "would be ideal" in line 101.

11-1. Page 7, line 100: please provide the latitude of the site

11-2. Line 106: 'The MRI wind profiler' => 'The MRI 1357-MHz wind profiler'

11-3. Line 113: see my previous remarks about w (p. 4)

Response:

11-1. We have added the latitude of the site in Table 1.

11-2. We added the frequency in the manuscript (lines 128–129): "The profiler used in this study operated at 1357.5 MHz with 100 m pulse lengths".

11-3. Please see our response #3-1.

12-1. Page 8, line 119: 'In the experiments' => 'For the experiment purpose'

12-2. Line 122-123: about pseudorandom frequencies. This is either too much or not enough explained for a non-expert reader. Is it necessary to mention? I suggest to move this specificity to Table 1.

Response:

12-1. Done (line 142).

12-2. We have copied this term to Table 1 but also added an explanation for this term to respond to the comment (lines 150–152): "The frequency sweeps were randomly shuffled within each frequency range to make acoustic spectrum almost uniform (Angevine et al., 1994)".

13-1. Page 9, line 134-137: am I right to say that the beamwidth of the speaker should be larger than the MRI beamwidth? Does that mean that you start with degraded conditions with the default sound beam? Is it the point you raised when you spoke of the parametric speaker directivity (line 22, page 2)? I raise this point since I wondered at the beginning whether the directivity would be an advantage or a drawback.

13-2. Line 137: turbulence will broaden the sound beam width, especially inside the boundary layer, but it will also reduce the measurement range, as you said before.

13-3. Line 137: 'aloft' is not accurate enough and I wonder whether it is appropriate here.

Response:

13-1. We believe that the beam width of the speaker should match that of profiler, because if the former is much narrower than the latter, no RASS echo is observed. On the other hand, if the former is larger than the latter, the height coverage is reduced because of decrease of the peak power as shown in Fig 2. We have added an explanation to respond to this comment (lines 162-168): "Prior to the designing of the MRI PAA, we made…".

13-2. The reviewer is right. However, we expect that the size of the sound spot matches the width of the radio wave width by the beam broadening due to turbulence. We have added an explanation to respond to the comment (line 172): "and match the radio beam width".

13-3. We have removed "aloft" (line 171).

14-1. Line 138: 'measured in the field' I would add: 'with a sound level meter'.

14-2. Could you describe the measurement protocol?

Response:

14-1. Done (line 175).

14-2. We have an explanation of the protocol to respond to this comment (lines 173-180): "In order to measure the audible sound pressure level…" .

15. Line 143: 'and is **therefore** significantly more annoying' (therefore can be added if you find it relevant).

Response: We have added the term in line 186.

16. Page 11, line 161: at 10-m height?

  Response: This was typo as the reviewer pointed out, and we have revised the manuscript to respond to this comment (lines 203–204): "at 20 m AGL".

17-1. Lines 163-167 : my first reaction is that the launching occurred in a period of the day when the time temperature gradient is important and the boundary layer top level is rapidly increasing. You discuss this point later on, but you could already add a few comments.

17-2. I also suggest to add a column in Table 3, with the time difference between the launching and the sunrise time. I calculated 2h30 to 4h. Am I right?

Response:

17-1. We have revised the manuscript to respond to this comment (line 205): "which may be preferable for the formation of inversion layer".

17-2. Since the analysis of the inversion layer evolution is beyond the scope of the present study, we did not provide the sunrise time for all the experiments in Table 3 but added it just for a sample profile for Fig. 8 (line 372): "This observation was made more than 3 h after sunrise (05:15 JST) on that day." Yes, the reviewer's estimation time was right.

18. Line 170: I do not understand the meaning of 'availability'. Do you mean 'practical relevance'?

Response: We have replaced "availability" with "applicability" (line 215).

19. Page 12, line 182: tell me if I am wrong, but it seems to me that the reference (ISO 1993) is not easily available. Could you provide (in an appendix) the equations to calculate the sound attenuation coefficient and the attenuation, derived from the RS measurements?

  Response: The reference is available online at: https://www.iso.org/standard/17426.html. However,

we have added a derivation of equations and some results in an appendix to respond to this comment.

20-1. Page 13, line 200: 'the PAA also reached a minimum altitude of 1.1 km AGL' => 'the PAA reached an altitude of 1.1 km AGL'.

20-2. Lines 203-206: this unique example is not enough to draw a conclusion. So, I would use 'may reach' instead of 'can reach' and indicate that the propagation level will be systematically compared between the 2 systems. or, you can simply say that the example in Fig. 4 is promising....

Response:

20-1: Done (line 246).

20-2: We have replaced "can reach" with "may reach" in line 250, and added "The height coverage of the two speaker systems are discussed later." in lines 252–253 to respond to this comment.

21. Fig. 5: usually, the backscattered signal of wind profiler radars is artificially corrected at the first gate to avoid receiver saturation. Are you sure it is not the case for RASS systems? Could this be a reason for the increase of the echo power between the first and the second gate?

Response: We think that the reviewer is talking about the STC. Our wind profiler does not implement the STC since it is equipped with an A/D converter with wide (16-bit: 96dB) dynamic range. We believe the increase between the first and the second gate were caused by other reasons, as Lataitis (1992) pointed out. We have added an explanation to respond to this comment (lines 311–314): "factors including the recovery of the receiver and incomplete overlapping of the electromagnetic and acoustic beams due to the special separation between the antenna and speaker systems could lead to a significant gradient in the receiving power at this gate (Lataitis, 1992)."

22-1. Page 15, line 228: 'available' => 'convenient'

22-2. Line 231: 'immediately'=> 'sharply'

Response:

22-1. We have replaced "available" with "applicable" in line 287.

22-2. Done (line 290).

23-1. Fig. 6: I suppose your sample of profiles is the best you could provide. Would it be possible to have a look on the corresponding Received Power profiles?

23-2. Why is there such a large difference in the number of data (320 and 237 in Fig. 6a) while the measurement range is the same for both systems? On the opposite, in Fig. 6d, 96-90=6 is small while the PAA vertical range is 200 m lower than the acoustic speaker. I probably miss something.

23-3. I suppose you tried comparisons with RS data averaged during 15 min or 30 min. Were the results so bad?

Response:

23-1. We have added profiles of P_r in Fig. 6, and an explanation to respond to this comment (lines 317–321): "It is noteworthy …a received RASS echo power…".

23-2. This happens because the height coverage changes with time especially for the PAA as shown error bars in original Fig. 10. In that figure, the second left (2.1m/s) is the data for Fig. 6a. (see Table 3). The PAA has longer error bar than the ACS, showing wider variation of the height coverage. In contrast, for Fig. 6d (4th left, 3.1m/s in original Fig. 10), the error bars are relatively short for each system indicating small variation of the coverage. The height coverage in Fig. 6 reflects the maximum height coverage in the RASS duration. Therefore, the number of the data has weak relation with the height coverage; rather, it is related to mean height coverage as written in lines 348–349. To avoid confusion, we have revised the manuscript (lines 438–439 and 461–464): "which (is =>) may also be reflected by the fewer number of data in the statistics", and "Note that the mean RASS height coverage shown in the figure is different from the height coverage of the mean virtual temperature profile in Fig. 6, because the latter reflects the maximum height coverage within the observed profiles after quality control in the duration of the RASS measurement."

23-3. We have tried to average for 30 min from 0815 to 0845. For instance, on 15 October, when there was no inversion layer aloft, the statistical results for 30 min mean, (bias, STD, N) = ACS(-0.19, 0.13, 165), and PAA(-0.18, 014, 124) were not very different from those for 60 min in bias (Fig. 6a). However, in the case of 8 November, when inversions were evident, the statistics, ACS(-0.13, 0.26, 152) and PAA(-0.81, 0.32, 106), became worth in bias than that for 60 min (Fig. 6c). Standard deviations were slightly improved by averaging over 30 min for both cases because it may reflect the time evolution of the temperature profile. However, the maximum height coverage for PAA reduced 100 m (one gate) by decreasing mean time for both cases although those for the ACS did not change.

24-1. Page 16, line 245: '(e.g. Figs 6n and 6c)' => 6a also.

24-2. Line 249 : I suggest that you give here the reason for the range corrections presented by Görsdorf and Lehmann and that you briefly explain the processing.

24-3. The range corrections should be applied to the whole profile (and not only at the first gate), to mitigate the discrepancies at the inversion levels.

Response:

24-1. Done (line 309).

24-2. We have added an explanation to respond to the comment (lines 314–317): "In addition, a range error (e.g., Angevine and Ecklund, 1994; Görsdorf and Lehmann, 2000; Johnston et al., 2002) caused by the height variation of the backscatter intensity may also contribute to the smaller received power."

24-3. We have revised the text as mentioned above (#24-2) and in lines 387–388: "… the discrepancies in and below the inversion could be mitigated by … **applying a range correction**.

25. Lines 251 to 253 (page 16, 'The RASS data were averaged for about an hour. The RS data were smoothed by 100 m running means to match the RASS observations)' should be moved p15, just before the comments on Fig. 6.

Response: Done (line 301).

26-1. Page 18, line 278: as said before for Fig. 6, I'm not convinced by the argument of the link between the smaller data number for the PAA and the height coverage. In addition, the wind is relatively stronger at 1300m in Fig. 5a, while the height coverage is similar for both systems.

26-2. However, I also find it necessary to discuss the effects of time evolution on the temperature profiles and of wind.

Response:

26-1. Please see our response #23-2.

26-2. We have added an explanation to respond to this comment (lines 464–466): "The long error bars may reflect the large time evolution of the RASS height coverage, which may also be related to the evolution of the wind in the duration."

27-1. Page 19, line 296: what is the standard deviation of the temperature increase?

27-2. Line 297: 'In this case' is awkward.

Response:

27-1. We have added "with a standard deviation of 1.0°C" in lines 366–367.

27-2. We have replaced " In this case" with "Thus" in line 367.

28. Lines 298-300: The comparison with the RS is good for an average of one-hour and you well explain that such an average is necessary to mitigate the errors due to the lack of the vertical velocity measurement. I agree that there are several reasons that could explain the RASS standard deviation during one hour, but that should not affect the average (unless surface covers or advection processes would be drastically different between the RS launching site and the RASS site). So what do you mean by 'degrading the statistics'? Increasing the standard deviation?

Response: We mean that an average period may affect not only the standard deviation but also the bias by "degrading statistics". For instance, 10 min mean Tv [°C] observed at 1.2 m AGL from 08:00 JST for 1 hour on 15 October 2016 were as follows, (08:00, 14.175), (08:10, 14.900), (8:20, 15.840), (8:30, 17.185), (8:40, 17.158), (8:50, 17.572), and (9:00, 18.142). The mean for this hour is 16.42°C at 08:30 but this value may change with averaging period (Note 17.19°C was observed at 08:30). Although they are values observed near the ground, we believe that an average period may affect the bias and would like to retain "degrading the statistics" in the text (line 370).

29. Pages 19 and 20 and Fig. 8:

Are the 1-hour profiles of the RASS centered around 30 min after the RS launch (8h30 in the caption of
Fig. 8)? Why did not you center them on the launch time since you are interested in the low layers?

Response: We centered the RASS duration on the launch time; The RSs were launched not at 08:00 JST
but at 08:30 JST as written in line 201, and the most of RASS durations were from 08:01 to 09:00 to
center the RS launch as shown in Table 3.

30-1. I do not find that the 1min-RASS profiles in Fig. 8 are closer to the RS profile than the RASS
1-hour average. It is true for some points, but not for all and it is not surprising:

30-2.   I think it is not significant to compare the 1-min RASS profiles to the RS profile since 1-min
RASS estimations include fluctuations (temperature fluctuations and fluctuations linked to the
measurement process). 1-min is too short to include enough time (or space) scales of turbulence. So
the 1-min profiles reveal some snapshots, which could be very different, 2 min later and a fortiori,
different from a RS profile, measured 400-m apart (in addition to the fact that the radiosonde takes
around 3.25 min to reach 1300 m).

30-3. It could be interesting to check the time evolution of the RASS profiles during the hour. Would this
evolution seem erratic like in a turbulence process? Or could we see a slow increase of the inversion
layer? (I do not require that you include this in your next manuscript, but it could be interesting to
discuss this point).

30-4. As far as the inversion levels are concerned, I tried to join the points of the 1-min profiles in Fig. 8.
The first inversion level that is detected at around 650 m with the RS is found at around 520 m and
500 m by the acoustic and parametric speakers respectively. This discrepancy could perhaps be
decreased by a range correction, but there again, you could not conclude due to the lack of vertical
velocity information (that can hardly be neglected when two successive 1-min profiles are compared).

Response:

30-1. We have revised the text to respond to the comment (lines 378–380): "By contrast, the 1 min raw
RASS data recorded around the radiosonde launch time represented the inversion layer better than the
mean RASS measurements **at some points**".

30-2. As reviewer pointed out, 1-min is too short to include the time and space scales of turbulence and
causes large error, if the temperature fluctuation due to turbulence is very large. However, in that case,
the radiosonde data sampled at 1 s cannot be used as a standard reference temperature measurement
because the mean time for radiosonde observation at each height is less than 17 s even after applying
100 m running means. Since there are some conformities between the radiosonde and RASS in
measuring Tv profiles, we believe (and assume) the temperature fluctuation due to fluctuation was
small and averaged out to some extent. We have revised the text to take the effect of turbulence into

account and to respond to this comment (lines 303–304 and 380–382): "The running mean may also play a role to mitigate the effect of the temperature fluctuation due to turbulence on the radiosonde measurements.", and "which may have been due to the locality of the inversion layer, the effects of vertical air motion or **turbulence**, ...".

30-3. We have tried to make a time-height cross section of Tv (Fig. 1R) just for the reviewer. Although a cold layer, which was a component of the inversion layer, was analyzed at about 600 m AGL from 08:05 JST (or before), the layer is evanescent in the figure. On the other hand, since the temperature observed at surface did not fluctuate as is seen at low altitudes (200 – 400 m AGL) in this figure, this fluctuation was not true but was likely biased by the vertical air flow. Thus, we expect that a long-lived cold layer would be analyzed longer in time if the correction for the vertical component of the wind can be applied. However, since it is beyond the scope of this study, we do not think it is interesting to discuss the evolution of the inversion layer with this figure.

30-4. We have added an explanation to respond to the comment (lines 387–388): "the discrepancies in and below the inversion could be mitigated by considering the effect of the vertical airflow and/or **applying a range correction**."

31. Nonetheless I agree with your conclusion p. 20: 'a comparison with measurements that have both small spatial difference and high time resolution is needed to evaluate the PAA-RASS measurements.'

Response: We appreciate the reviewer's comment on this.

32. Page 22, lines 341 to 345: I do not agree with these arguments since they describe atmospheric phenomena whose time scales are larger than 1 min. I think, as said before, that the variability comes from the local turbulence and also perhaps from the physics of measurement that is probably different between the 2 systems. Could the difference in the beam widths play a role? The fact that the standard deviation (0.43) in the 1-min statistics of PAA vs acoustic is around the same as the standard deviation (0.4) of the 1-hour statistics of both RASS vs RS reinforces the idea that small scale processes are responsible for the variability (in addition to processes at larger scale like the increase of the inversion levels with z and time).

Response: We agree that the standard deviation (0.43) in the 1-min statistics of PAA vs. acoustic could be mostly due to local turbulence since the spatial difference was negligible and the time difference was quite small as the reviewer pointed out. We have revised the text to respond to this comment (lines 415–417 and 564–565): "Since the spatial difference was negligible and the time difference was quite small, the reason for this discrepancy could include **temperature fluctuation due to turbulence**.", and "temperature fluctuation due to turbulence could contribute to deteriorate the statistics." We do not think that the difference in the beam width play the role (as long as temperature is horizontally homogeneous, which we assumed in comparisons with radiosondes).

10

33-1. Page 23, line 364: see my questions about Fig. 6 (p. 15)

33-2. Line 368-369: I do not understand:' On the other hand, the results also suggest that the reason may include the effect of wind aloft (e.g. Fig. 5a)' since the height coverage is the same for this specific case.

33-3. Line 369: 'wind aloft' should be defined here and not p. 24, lines 364-365.

33-4. Are you sure wind is measured at 1 m? (1 to 1200 m AGL). How did you compute the standard deviation of the wind?

Response:

33-1. Please see our response # 23-2.

33-2. See our response # 23-2. We have also revised the manuscript to avoid confusion (lines 293-295): "This suggests that the PAA **has enough peak power to reach the highest range gate but** is more susceptible to high winds than the acoustic speakers".

33-3. We would retain the location of the definition of "wind aloft" in line 456, because this range is defined just for Fig. 10, which is introduced first in line 452.

33-4. This was a typo, and we have corrected (lines 456–457): "the mean wind from **20** to 1200 m AGL (Table 3)". The standard deviation of the wind speed in Table 3 was derived from the radiosonde data by

$$\sigma = \sqrt{\frac{1}{N}\sum_{i=1}^{N}(x_i - \bar{x})^2}$$

, where x_i is the observed i^{th} wind speed data from the beginning of the observation, and the altitude of the Nth data is the closest to but less than or equal to 1200 m AGL.

34. Page 24, line 384: the linear regression for the acoustic speaker is not relevant. I would remove it from Fig. 10.

Response: We have revised Fig. 10 based on the reviewer's comment # 47-2.

35. Lines 388-389: 'This suggests that the acoustic speaker RASS **keeps on observing** at a high altitude **even** in relatively high wind conditions.'

Response: Done (line 477).

36-1. Page 27, line 423: 'may be distorted' => 'may have been distorted'.

36-2. Line 424 : 'may be needed to be steered' => might have been steered'.

Response:

36-1. Done (lines 515–516).

36-2. Done (line 516).

37. Page 29, line 455: 'does' should be removed.

Response: Done (line 574).

38. Page 30, line 473: I do not understand 'but frequency is likely to be less'.

Response: This term (line 592) means the frequency of the occurrence in other seasons, not the frequency of the acoustic and/or radio wave.

39. Additional question: does an emission around 40 kHz require an authorization?

Response: There is no requirement for authorization at least in Japan. However, there are some recommendations from organizations including WHO. We have added Section 4.4 to respond to this comment.

40. As a conclusion, I would be pleased to see your future works with this system, with more favorable conditions such as: the possibility to measure w, some range corrections, measurements during the whole day. I am still wondering whether the parametric system would be more efficient than the acoustic system at inversion layers (due to its narrower bandwidth).

Response: We thank the reviewer for his/her positive conclusion.

41. Table 3: I would use U instead of W (even if W is not w) and would add '(1 to 1200 m AGL)' after 'wind aloft'.

Response: Done (Table 3).

42. Figure 5: 'except for the first range' => '(except for the first range)'.

Response: Done (Fig. 5).

43-1. Figure 6: 'from 08:30 JST' is not convenient for the 4 profiles. See also my previous remark about Fig. 8, concerning the center of the 1-hour time average.

43-2. 'The error bars represent 2 σ in the RASS hourly observations' ('hourly' added).

Response:

43-1. Please see our comment #29; The RSs were launched not at 08:00 JST but at 08:30 JST in Japan.

43-2. Done (Fig. 6).

44. Figure 7: I would say RASS vs. radiosonde instead of radiosonde vs. RASS, but the editor will confirm or refute.

Response: Done (Fig.7).

45. Figure 8:'RASS with acoustic speakers (red) between 8h01 and 8h02' 'RASS with parametric speaker (blue) between 8h02 and 8h03'

Response: Since radiosonde was launched at 08:30, we did not change the time for the RASS measurement. Instead, we have revised the text to make it clear (Fig. 8): "closed circles represent 1 min raw data **from the time indicated**."

46-1. Figure 9: Same remark as in Fig. 7 for the use of vs.

46-2. '(except for the first gate)'

46-3. 'a normalized frequency diagram (**color scale**)'

46-4. 'the mean **hourly** data were plotted in (b)'

Response:

46-1– 46-3. Done (Fig. 9).

46-4. We have replaced "mean data" with "hourly-mean data (Fig. 9).

47-1. Figure 10: 'wind speed aloft **(1-1200m)**'

47-2. Please remove the linear regression for the acoustic speaker or present two legs: one horizontal from 1.5 to 5.5 m/s and another oblique one for stronger winds.

Response:

47-1. We have replaced "aloft" with "aloft (20–1200 m AGL)" in Fig. 10.

47-2. Done in Fig. 10. However, we have replaced the mean wind speed aloft with the horizontal displacement for the horizontal axis.
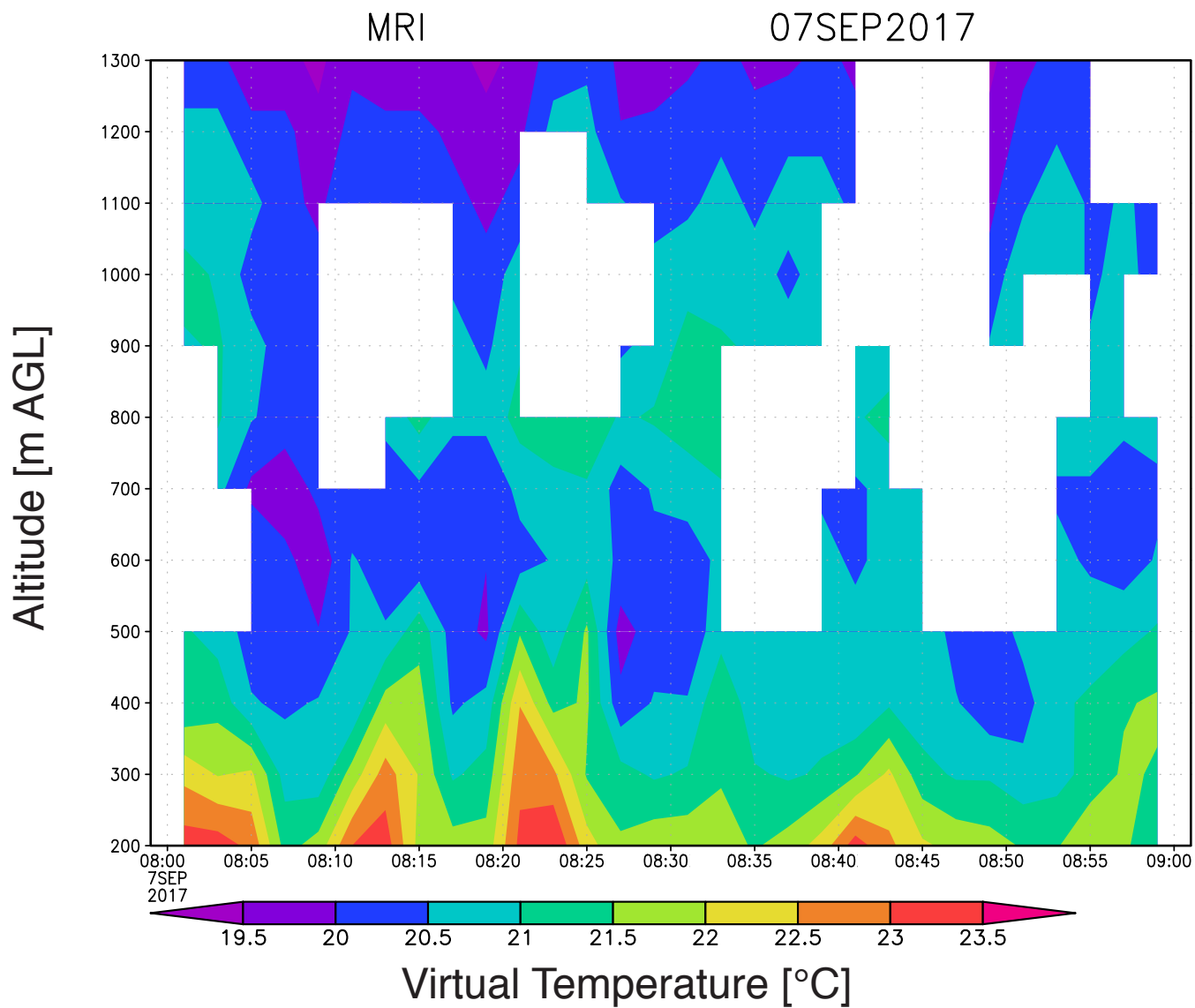
Fig. 1R. Time height cross section of virtual temperature obseved with RASS averaged over 2 min.

Response to Reviewer 2

We are grateful to the reviewer for the very careful and thorough examination of our manuscript. We think the revised manuscript is substantially improved as a result.

Specific Comments:

1. Line 54: In order to get the true acoustic speed in a particular antenna beam direction, the radial wind speed should be subtracted from the measured acoustic speed. Therefore, "vertical wind" should be replaced with "radial wind".

Response: We have replaced "vertical wind" with "radial wind" in lines 50, 54 and 56.

2. Lines 138-144:

2-1. The sound pressure level (SPL) output of the PAA in the audible range is given in dB. It would be better to give the reference to weighting curve e.g. dBA or dBZ to make it more explicit.

2-2. In figure 2, the SPL is measured at a distance of 25 m from the PAA. As the general practice of measuring SPL for an acoustic source is at 1 m above the source, the reason for measurement having been done at 25 m should be explained.

2-3. Why is the SPL of PAA not available in the elevation angle range of $0° - 40°$. This measurement is of high relevance as the unique advantage of PAA is high directivity (meaning low transmission along the horizon when transmitting vertically). Effort should be made to provide these measurements.

Response:

2-1. We have added "dBA" (line182): "the SPL was less than 55 dB (**dBA**) at a zenith angle of 40°"

2-2. We have added an explanation to respond to this comment (line 174): "The measurements were made … at a distance of 25 m, because a range of 10 m would be necessary to complete producing audible sound from ultrasound with a PAA of this size (Prof. Kamakura, 2018, personal communication). Safety was also considered for the level-meter operators in determining the distance, as is discussed later."

2-3. We have revised Fig. 11 to show the SPL of the PAA.

Section 3.1 :

3. Lines 175-177: It is stated that "the PAA radiates bifrequency primary waves that are around 37 kHz and 40 kHz". However, Table 2 indicates Amplitude Modulation (DSB). It is not clear if these two frequencies were generated simultaneously by two halves of the PAA or the 40 kHz was modulated with the desired audio frequency. This should be clarified.

Response: The reviewer is right. The term DSB in the original Table 2 was wrong and removed. (We

don't think that the AM works well for RASS because ultrasound, the carrier, cannot propagate long distances.)

The two frequencies were generated simultaneously by all transducers of the PAA. To avoid confusion, we have revised our manuscript (lines 219–222): "The MRI PAA radiates bifrequency primary waves that are around 37 kHz and 40 kHz from all the transducers **simultaneously** to generate the parametric sound".

4. Further, it is stated in line 122 that pseudorandom frequencies were chosen. What is the range of frequencies and how were they sequenced.

Response: We have added an explanation for this comment (lines 145–152): "Prior to every experiment, an acoustic wave with a wide frequency range (2715 to 3265 Hz corresponding to about ±50°C) was generated to detect center Doppler frequency of the RASS echo. Then, during each experiment, the emitted acoustic frequency range was automatically narrowed down to a shorter frequency span (130 Hz, corresponding to about ±12°C) around the detected center frequency to increase SNR and height coverage. The frequency sweeps were randomly shuffled within each frequency range to make acoustic spectrum almost uniform (Angevine et al., 1994)."

5. The ultrasonic SPL generated by the PAA is 200 dB which is extremely high. As per several studies (cf.[1] and [2]) physiological effects start manifesting in small animals at 120 dB and increase in severity with increasing SPL; exposure above 180 dB, death of a human could occur. Observations of insect, animal or bird mortality in the vicinity of the PAA should also be mentioned. Instances of hearing loss or any other discomfort faced by operators exposed to the PAA should be mentioned for the benefit of prospective users. In view of the high potential for biological hazard from this speaker, the paper should clearly mention the potential for harm from these high levels of ultrasound and give references to internationally accepted safety procedures to be adopted while using high power ultrasonic sources.

Response: We have added Section 4.4 for this comment. We have also added some considerations for safety in the revised manuscript (e.g., line 178 and Fig. 1d). We thank the reviewer for this comment and providing the references.

6. Section 4.3: The effect of horizontal wind on the height coverage can be estimated using acoustic ray tracing. Therefore, it is recommended that the discussion about height coverage should be given with reference to the ray tracing results.

Response: We have estimated the horizontal displacement of the sound from the radio wave by using acoustic ray tracing and revised Figs. 5 and 10 to discuss the effect of horizontal wind on height coverage in Section 4.3.

7. Line 408: How was the power decreased by 15 dB – by reducing the input drive or by using smaller aperture. This clarification should be added.

Response: The decrease in line 497 was not made manually but associated with the beam broadening as written in the same line. On the other hand, the peak power was reduced manually in measuring the SPL at multiple zenith angle (Fig. 11). We have added an explanation for this comment (line 503): "The peak power was decreased by about 7.5 dB by reducing the power supply to the PAA amplifier, which decreased not only the audible sound but also the ultrasound levels for practical reasons (noisy) and measurement safety."

Minor corrections

8. Line 80: Replace "is expected" with "would be ideal".

Response: Done (line 101).

9-1. Line 86: Replace "audible frequencies" with "frequencies in the audible range".

9-2. Line 88 : Replace "Hence after" with "Thereafter".

Response:

9-1. Done (line 106).

9-2. Done (line 109)

10. Line 107: Add "and" between Oceanic and Atmospheric

Response: Done (line 127).

11. Line 124: Replace "comprised" with "consists of".

Response: Done (line 153).

12. Line 136: Replace "broaden" with "broadened".

Response: Done (171).

13. Line 199: Replace "reached" with "were obtained from altitudes"

Response: Done (line 245).

14. Line 200: Replace "also reached" with "were obtained from"

Response: We have modified the text to response to a comment from another reviewer (line 246): "the PAA reached an altitude of 1.1 km AGL".

15. Lines 396- 399: The sentence need to be rewritten. I suggest as follows,

"Since the four acoustic speakers were not adjusted in phase, this robustness could be explained by the higher aggregate sound power than that shown in Fig. 2 and possible location of sound waves above the antenna in spite of relatively high winds."

Response: Done (lines 485–488). Thank you.

16. Line 429: Replace "availability" with "applicability".

Response: Done (line 546).

1

Application of Parametric Speakers to

Radio Acoustic Sounding System

2

3

4

by

5

Ahoro ADACHI[1] and Hiroyuki HASHIGUCHI[2]

6

7

[1]Meteorological Research Institute, Japan Meteorological Agency

8

1-1 Nagamine, Tsukuba, Ibaraki 305-0052, Japan

9

[2] Research Institute for Sustainable Humanosphere, Kyoto University

10

Gokasho, Uji, Kyoto 611-0011, Japan

11

12

Correspondence to: Ahoro ADACHI (aadachi@mri-jma.go.jp)

13

Tel: +81-29-853-8584 / Fax: +81-29-856-0644

14

17

Abstract

In this study, a wind profiler with radio acoustic sounding system (RASS) and operational radiosonde measurements were used to investigate the technical practicability and reliability of using parametric speakers to measure the vertical profile of virtual temperature. Characteristics of parametric speakers include high directivity and very low sidelobes, which are preferable for RASS, especially those operating at urban areas. The experiments were conducted on fine days with light winds to mitigate the effects of the horizontal and vertical components of wind on acoustic waves used for RASS. The results of this study indicated that, although parametric speaker RASS is susceptible to horizontal winds due to the narrower acoustic beam, bias and standard deviation of parametric speaker RASS versus radiosonde virtual temperature difference (0.1°C, 0.4°C) were close to that from acoustic speakers (0.0°C, 0.4°C). In addition, when compared with acoustic speaker RASS, the values for the parametric speaker RASS were even smaller (0.1°C, 0.2°C). Based on these results, it is concluded that the parametric speaker RASS has accuracy and precision comparable with acoustic speaker RASS despite its high directivity of sound.

34

1 Introduction

36 Accurate measurements of temperature are essential in weather forecasting and studies

37 of atmospheric dynamics at all scales. The radio acoustic sounding system (RASS) is a

38 ground-based remote sensing technique that provides vertical profiles of virtual

39 temperature from a few hundred meters above the surface up to several kilometers in

40 elevation (Marshall et al., 1972; Peters et al., 1985). RASS technique has been applied

41 to wind profilers, whereby vertical profiles of virtual temperature can be measured with

42 the same temporal and spatial resolution that the profiler uses to measure winds (e.g.,

43 Adachi et al., 2005) with a relatively high degree of reliability (Matuura et al., 1986;

44 Moran et al., 1991; Angevine and Ecklund, 1994).

45   When using RASS techniques, one or more acoustic sources are co-located with

46 an antenna, and the profiler provides the vertical profile of the speed at which the

47 acoustic disturbance propagates vertically (Angevine et al., 1994) from the

48 measurement of Doppler spectrum. RASS temperature measurements can be obtained

49 on the basis of the relationship between the virtual temperature T_v (°C), the local speed

50   of sound C_a (m s^{-1}) and the measured radial wind speed w (m s^{-1}), and a good

51   approximation can be obtained by

52    $$T_v = \left(\frac{C_a - w}{20.047}\right)^2 - 273.15. \qquad (1)$$

53   Thus, a vertical profile of the speed of sound can be converted to a profile of virtual

54   temperature. The radial wind speed is considered in Eq. (1) because the neglect of the

55   wind velocity along the beam is the largest source of error in RASS measurements (e.g.,

56   May et al., 1989; Angevine et al., 1994). However, we do not consider the radial wind

57   speed in our experiments, because strong clutter sometimes contaminates the Doppler

58   spectrum and masks the atmospheric echo in the vertical beam observation. This issue is

59   addressed in later sections.

60   The systematic error or bias of the virtual temperature measurements from RASS

61   observations have been shown to be less than 1°C, while the standard deviation or

62   precision has also been reported around 1°C. May et al. (1989) compared virtual

63   temperatures obtained from 915 and 50 MHz RASS with those obtained from

64   radiosonde measurements. The RASS data was averaged over approximately 6 min, and

65   about 50 soundings covering both the summer and winter seasons were examined. Both

66   the bias and the standard deviation were about 1°C, even without the application of the

67   vertical velocity correction. On the other hand, Martner et al. (1993) assessed the

68   performance of 915, 404 and 50 MHz wind profilers with RASS by comparing with

69   about 150 radiosonde measurements. They found that the bias (standard deviation) was

70   less than 0.3°C (about 1°C) for most systems, even though they did not make the

71   correction for vertical air motions, as the comparison was made under low vertical wind

72   conditions. Moran and Strauch (1994) compared temperature profiles obtained using a

73   VHF wind profiler with RASS with those obtained from radiosondes during a 5-week

74   period. They reported that the accuracy (standard deviation) was 0.9°C (less than 1°C),

75   after the application of the vertical velocity correction. Moreover, Angevine et al.

76   (1998) compared the virtual temperature measured by a 915 MHz wind profiler with

77   RASS with *in situ* observations at 396 m AGL on a tower. They found that the precision

78   of the RASS measurements was less than 0.9 K after the application of the vertical

79   velocity correction and corrections for thermodynamic constants. In addition, Görsdorf

80   and Lehmann (2000) reported that the bias (standard deviation) of the RASS

81   measurements with a 1.3 GHz wind profiler is 0.1K (0.7K) from the data observed for a

82 year compared with radiosondes if accurate corrections for vertical velocity, range, and

83 thermodynamic constants are applied. On the other hand, the height coverage of RASS

84 depends on the radio wave frequency deployed (May et al., 1988; Martner et al., 1993)

85 but is also limited by both the advection of the sound wave with the horizontal wind and

86 the atmospheric attenuation of the acoustic signal in addition to the effects of turbulence

87 and vertical temperature gradients (Lataitis, 1992).

88   A wind profiler with RASS has been frequently used to study the dynamics of the

89 atmosphere, especially in the boundary layer (e.g., Neiman et al., 1992; Peters and

90 Kirtzel, 1994; May, 1999; Bianco and Wilczak, 2002; White et al., 2003; Adachi et al.,

91 2004; Hashiguchi et al., 2004; Chandrasekhar Sarma et al., 2008). Among the

92 limitations of this method, an important one is the emission of strong sound waves,

93 whose frequency cannot be arbitrarily selected, but determined by the wavelength of the

94 radio wave used by the profiler to match the Bragg condition (the acoustic wavelength

95 λ_a is equal to half the electromagnetic wavelength λ_e). Although the acoustic speakers

96 used for RASS measurements are usually co-located with the antenna and directed

97 vertically so that the generated sound wave propagates along the radio wave, a large

98 portion of the sound wave leaks horizontally because of the sidelobes of the speakers,

99 which prevents the temporal and/or continuous operation of RASS in urban

100 environments (Wulfmeyer et al., 2015). Thus, a new type of speaker that has extremely

101 low sidelobes would be ideal for RASS measurements.

102   A theoretical study of parametric speakers (or parametric acoustic array, PAA)

103 was established by Westervelt (1963). That study revealed that the nonlinear interaction

104 between two collimated high-frequency sound beams in an ideal fluid medium produces

105 two new waves with a sum and difference frequencies, and the latter may be used to

106 produce narrow beams of sound at relatively low frequencies in the audible range.

107 Berktay and Leahy (1974) presented a theoretical description that can be used to

108 compute the far field response of a parametric array for multiple sets of parameters.

109 Thereafter, the use of parametric arrays underwater has been the subject of a number of

110 theoretical and experimental studies. On the other hand, an experimental investigation

111 of the parametric array in air was first demonstrated by Bennett and Blackstock (1975),

112 and recently, the parametric loud speaker has become available for audio and speech

113 applications (Gan et al., 2012). The properties of parametric speakers include high

114 directivity and very low sidelobes, which are preferable for RASS measurements.

115 However, to the best of our knowledge, there are few, if any, studies on RASS

116 techniques using this type of speaker.

117 In this study, a detailed evaluation of the parametric speaker for RASS

118 measurements was conducted by comparing temperature data derived from this type of

119 speaker and those from both radiosonde and acoustic speaker RASS at the

120 Meteorological Research Institute (MRI) field site in Tsukuba, Japan. Instrumentation

121 and data analysis techniques are presented in Section 2. Results are presented in Section

122 3 and discussed in Section 4. Finally, a summary of our conclusions are presented in

123 Section 5.

124

125 **2 Instrumentation and data analysis techniques**

126 The MRI wind profiler, a four-panel LAP-3000 with RASS (Fig. 1a), is the type

127 originally developed at the National Oceanic and Atmospheric Administration (NOAA)

128 Aeronomy Laboratory (Carter et al., 1995; Ecklund et al., 1988). The profiler used in

129 this study operated at 1357.5 MHz with 100 m pulse lengths and a minimum

130 (maximum) gate of 200 m (1300 m) from the antenna in RASS mode. The vertical

131 resolution was set to 100 m based on the requirements for the Global Climate Observing

132 System (GCOS) Reference Upper-Air Network (GRUAN) by the WMO (2007). The

133 effect of the vertical air motion was not considered for RASS measurements in the

134 experiments because strong clutter caused by automobiles on a nearby highway

135 sometimes contaminated the Doppler spectrum and masked the atmospheric echo

136 (Adachi et al., 2004). Indeed, the vertical velocity correction can decrease the accuracy

137 of RASS in situations with calm wind and a lower reliability of vertical wind

138 measurements (Görsdorf and Lehmann 2000).

139   The configuration and operating parameters of the wind profiler with RASS are

140 summarized in Table 1. The antenna of the profiler was co-located with four acoustic

141 speakers in cylindrical enclosures and a parametric speaker, which was mounted on top

142 of a shed (Fig. 1a). For the experiment purpose, the RASS measurements were made

143 continuously for about an hour without wind observations. Since the wind profiler

144 operated at 1.3 GHz, the frequency of the acoustic source for the RASS measurement

145 was set at about 3 kHz to match the Bragg condition. Prior to every experiment, an

146 acoustic wave with a wide frequency range (2715 to 3265 Hz corresponding to about

147 ±50°C) was generated to detect center Doppler frequency of the RASS echo. Then,

148 during each experiment, the emitted acoustic frequency range was automatically

149 narrowed down to a shorter frequency span (130 Hz, corresponding to about ±12°C)

150 around the detected center frequency to increase SNR and height coverage. The

151 frequency sweeps were randomly shuffled within each frequency range to make

152 acoustic spectrum almost uniform (Angevine et al., 1994).

153   The MRI parametric speaker, 100FM-001, consists of an array of more than

154 10,000 piezoelectric ceramic transducers configured on a semi-circular board with a

155 diameter of 1.8 m (Fig. 1b). The transducers were divided into 278 segments, with each

156 one mounted on the hexagonal board (Fig. 1c). The FPGA modules in the speaker

157 system were used to control the phase of the signals fed into the segments to generate

158 the acoustic beam with a particular preferred width and direction like other PAAs (e.g.,

159 Wu et al., 2012). The configuration and operating parameters of the speaker are

160 summarized in Table 2.

161   One of the desirable features of the PAA for RASS measurements is high

162 directivity of the sound beam. Prior to the designing of the MRI PAA, we made a

163 preliminary field sensitivity test for RASS using a prototype PAA with a beam width

164 smaller than 2° and relatively small power, but no RASS echo was observed. We

165 modified the prototype to broaden the beam width to about 6° or more, and the RASS

166 echo was observed up to a few range gates. We concluded that too narrow a beam is not

167 good for the RASS observation, and the PAA beam width should match that of the

168 profiler radio wave. Because the beam width of the MRI profiler is less than 7° (Table

169 1), the default sound beam width of the speaker was designed to be 5° (Table 2).

170 Although the latter width is somewhat smaller than that of the former, the RASS focal

171 spot determined by the sound beam width may be broadened by turbulence (Lataitis,

172 1992) and match the radio beam width, which is preferable for RASS measurements.

173   In order to measure the audible sound pressure level (SPL) pattern, we installed

174 the PAA on a flame (Fig. 1b) to radiate sound horizontally. The measurements were

175 made on fine (=no rain) days under calm wind (<2 m/s) with a sound level meter set at a

176 distance of 25 m, because a range of 10 m would be necessary to complete producing

177 audible sound from ultrasound with a PAA of this size (Prof. Kamakura, 2018, personal

178 communication). Safety was also considered for the level-meter operators in

179   determining the distance, as is discussed later. The PAA was installed on top of a shed

180   after the measurements (Fig. 1a). The audible sound pressure level (SPL) pattern (Fig.

181   2) measured in the field indicated that the PAA exhibited high directivity and low

182   sidelobes, as expected; the SPL was less than 55 dB (dBA) at a zenith angle of 40°,

183   which was close to the value of the background noise level of 50 dB despite the fact that

184   the peak power (100 dB) was close to that of an acoustic speaker (105 dB). By contrast,

185   for the acoustic speaker, the SPL was as high as 70 dB even at a zenith (elevation) angle

186   of 85° (5°) and is therefore significantly more annoying to the ear than a PAA.

187   To evaluate the parametric speaker for RASS measurements, temperature data

188   derived from the PAA-RASS were compared with values derived both from radiosonde

189   and from the acoustic speaker RASS. The dwell time for each RASS measurement was

190   set at about 57 s followed by an intermediate cessation operation time of 3 s, in which

191   the two speaker systems were alternately switched every minute for comparison. Each

192   RASS data set obtained with the two speaker systems was independently processed with

193   quality control to confirm the consistency in the height and time field values.

194   The profiles of virtual temperature derived from operational radiosonde

195   measurements were used as the standard reference data for comparison. The

196   radiosondes (the Meisei RS-11G used until September 2017, followed by the Meisei

197   iMS-100; Kizu et al., 2018) were launched from the Aerological Observatory, which is

198   located about 400 m northeast of the profiler (for the layout of the relative locations, see

199   Adachi et al., 2004). The time resolution of the radiosonde data used for the comparison

200   was 1 s, which corresponded to the height resolution of about 6 m. The radiosondes

201   were launched operationally at 08:30 JST (Japan Standard Time: JST=UTC+9 h), and

202   most of the RASS experiments included the launch time (Table 3). The RASS data were

203   taken during morning hours, on fine (= no rain) days, with light winds (< 3 m s^{-1} at 20

204   m AGL), mostly in autumn, when the region was under the influence of a high-pressure

205   system, which may be preferable for the formation of inversion layer. In the radiosonde

206   comparison, the RASS data were averaged over about an hour for each experiment to

207   mitigate both the effects of vertical velocity (Angevine and Ecklund, 1994; Görsdorf

208   and Lehmann 2000) and the spatial difference between the radiosonde and the profiler

209   with RASS. Using the hourly mean may also reduce the daytime downward bias (e.g.,

210 Görsdorf and Lehmann 2000; Adachi et al., 2005), which could be attributable to

211 insects or hydrometeors that are undetectable (Angevine, 1997). Contrastingly, the 1

212 min raw RASS data were used to compare the two speaker systems.

213

214 **3 Results of comparison**

215 **3.1 Applicability of parametric speaker to RASS**

216   As there are few, if any, studies on RASS using parametric speakers, preliminary

217 experiments were first conducted to confirm whether the secondary audible waves

218 produced by this type of speaker can propagate long distances along the radio wave

219 while satisfying the Bragg condition before evaluating it for RASS application. The

220 MRI PAA radiates bifrequency primary waves that are around 37 kHz and 40 kHz from

221 all the transducers simultaneously to generate the parametric sound of the secondary

222 difference frequency, which was around 3 kHz for RASS. Since sound absorption

223 generally increases with frequency, the ultrasound may be substantially dissipated as

224 altitude increases, although the peak SPL of the ultrasonic sound close to the PAA

225 (Table 2) was about 100 dB larger than that of audible sound generated by the acoustic

14

226   speaker (Fig. 2). The atmospheric absorption is a function of the sound frequency,

227   temperature, humidity, and pressure of the air (ISO, 1993). Example profiles of the

228   sound attenuation coefficient and attenuation at 3 kHz and 40 kHz derived from

229   radiosonde measurements are shown in Fig. 3. In the derivation, only the effect of

230   atmospheric absorption related to viscosity and thermal conductivity of the air,

231   molecular relaxation of rotation, and vibration of O_2 and N_2 was considered (see

232   Appendix), and other physical effects (e.g., reflection from the surface; ISO, 1996) were

233   disregarded. Figure 3a shows that the attenuation for the audible wave of 3 kHz

234   propagating from the surface to an altitude of 1 km above ground level (AGL) was 14.7

235   dB, which indicated that the sound wave at this frequency with an SPL of 105 dB on the

236   ground decreased to 90.3 dB at this altitude. By contrast, this figure also suggests that

237   the sound wave at 40 kHz with an SPL of 200 dB generated on the ground was reduced

238   to less than 0 dB at 160 m AGL. Thus, the primary wave of the PAA was not expected

239   to reach beyond this altitude. However, the difference-frequency component could

240   propagate to a higher altitude because it was audible sound.

241   Figure 4 shows a set of spectra obtained with the acoustic speakers and the PAA

242   at the time when the radiosonde measurement in Fig. 3 was made. The plots were

243   obtained by the LAP-XM, which is a software program developed on the basis of the

244   Profiler On-line Program (POP; Carter et al., 1995). The RASS echoes associated with

245   the acoustic speakers were obtained from altitudes as high as 1.3 km AGL. On the other

246   hand, those associated with the PAA reached an altitude of 1.1 km AGL. Although the

247   PAA-RASS height coverage was somewhat lower than that associated with acoustic

248   speakers, this was much higher than the altitude where the primary ultrasound waves

249   were expected to dissipate. This result suggests that the secondary difference-frequency

250   component may reach the altitude comparable with the audible wave generated by

251   acoustic speakers while satisfying the Bragg condition and propagating along the radio

252   wave as an audible wave. The height coverage of the two speaker systems are discussed

253   later.

254   Another conformity of the secondary audible wave formed by the PAA to the

255   sound wave by the acoustic speaker for the RASS measurement can be seen in the

256   vertical profiles of the received echo power. Samples of the RASS echo power profiles

257 are shown in Fig. 5, along with profiles of radiosonde wind speed and horizontal

258 displacement of the sound beam center for RASS from that of the radio wave. The

259 samples were selected from the days (Table 3) when surface winds were light (< 2 m

260 s^{-1}) except on 19 October (Fig. 5a). The displacement of the sound wave with horizontal

261 wind was estimated by acoustic ray tracing based on radiosonde measurements. In this

262 estimation, the sound speed was estimated using Eq. (1), assuming a stationary

263 atmosphere, in which the virtual temperature was obtained from the radiosonde data,

264 and the initial displacement of the PAA from the profiler antenna on the ground was set

265 at 4 m (Fig. 1a). The RASS echo power shown here is a relative value, not absolute,

266 because the profiler is not calibrated for received power.

267   The RASS echo power of both speaker systems decreased with altitude except for

268 the first range gate. The reason for the decrease may include atmospheric attenuation of

269 the acoustic signal and displacement of the acoustic wave from the radar antenna by the

270 wind (Lataitis, 1992), as shown by the displacement profiles (Fig. 5). The echo power

271 with the acoustic speakers was almost always larger than that of the PAA (Figs. 5a–5d).

272 This could be explained by the acoustic speaker's larger peak power than that of the

273   PAA (Fig. 2), and the integrated peak power of the acoustic system, which comprises

274   four speaker units (Fig. 1), could be much larger. ==The echo power with the PAA was==

275   ==slightly larger than that of the acoustic speakers at the first gate in Fig. 5a. This could be==

276   ==because the sound from the PAA was advected above the antenna as shown by no==

277   ==displacement at that height in the figure, suggesting that acoustic ray tracing was==

278   ==reliable.== The estimation of RASS echo power (e.g. Adachi et al., 1993) was beyond the

279   scope of this study. However, the echo power with both speaker systems in light-wind

280   conditions (Figs. 5b–5d) decreased almost linearly (in dB) with altitude above the first

281   gate, and the difference in the gradient between the two systems was relatively small

282   (less than 15 % on average), although this small difference may also be attributable to

283   the wind. From the facts mentioned above, we concluded that the secondary audible

284   waves formed by the PAA can propagate over a long distance along the radio wave

285   while satisfying the Bragg condition and are applicable to the RASS measurements as

286   the sound wave generated by the acoustic speaker.

287   Since the PAA was shown to be ==applicable to== the RASS measurements, we next

288   explored the reliability of the PAA-RASS measurements by comparing with radiosonde

289 observations. It is noteworthy, however, that in Fig. 5a, the echo power with the PAA

290 decreased with altitude more sharply than that associated with the acoustic speaker at

291 altitudes between 300 and 700 m AGL, where relatively high winds were observed,

292 despite the fact that the PAA-RASS echo reached the highest range gate (1300 m AGL)

293 as the acoustic speaker RASS. This suggests that the PAA has enough peak power to

294 reach the highest range gate but is more susceptible to high winds than the acoustic

295 speakers. Thus, the effect of wind on the PAA-RASS measurements is discussed later in

296 this paper.

297

298 **3.2 Comparisons with radiosonde**

299 Profiles of virtual temperature (Tv) derived from radiosonde, the PAA-RASS, and the

300 acoustic speaker RASS observations are shown in Fig. 6 along with the corresponding

301 statistics for the data. The RASS data were averaged over approximately an hour. The

302 radiosonde data were smoothed by 100 m running mean to match the RASS

303 observations. The running mean may also play a role in mitigating the effect of the

304 temperature fluctuation due to turbulence on the radiosonde measurements. The Tv

305 derived from the radiosondes was in good agreement with the RASS measurements

306   derived from both speaker systems, lying within the error bar of most of the range gates.

307   In addition, *Tv* derived with both speaker systems were close to each other. However,

308   bias and standard deviation tended to be large at inversion layers and at the first gate

309   (e.g., Figs. 6a, 6b, and 6c), the latter of which may corresponded to the smaller received

310   power at that gate as shown in Fig. 5. This could be attributable to the fact that the first

311   gate is too close to the antenna, and factors including the recovery of the receiver and

312   incomplete overlapping of the electromagnetic and acoustic beams due to the special

313   separation between the antenna and speaker systems could lead to a significant gradient

314   in the receiving power at this gate (Lataitis, 1992). In addition, a range error (e.g.,

315   Angevine and Ecklund, 1994; Görsdorf and Lehmann, 2000; Johnston et al., 2002)

316   caused by the height variation of the backscatter intensity may also contribute to the

317   smaller received power. It is noteworthy that the most of the highest range gates

318   correspond to a received RASS echo power of about −10 dB for both speaker systems in

319   Figs. 5 and 6, suggesting that the received power is one of the factors determining the

320   height coverage, although factors that determine the received power including the sound

321   attenuation may be different for each system.

322   Scatter diagrams comparing radiosonde virtual temperature with that from

323   RASS for all experiments are shown in Fig. 7 along with statistics. The first range gate

324   data of the RASS measurements were not considered because they are less reliable. This

325   figure shows that both the PAA and acoustic speaker RASS measurements of virtual

326   temperature were generally in good agreement with those derived from radiosonde

327   measurements, as expected. The linear regressions for both speaker systems were close

328   to the one-to-one relation, and correlation coefficients were close to unity. In addition,

329   the systematic error was less than 0.1 °C and the standard deviation was 0.4°C for both

330   systems, suggesting that both systems are reliable for RASS measurements.

331

332   **4 Discussions**

333   As reported above, we found many instances in which the PAA speaker system

334   exhibited comparable performance with the acoustic speakers with respect to the RASS

335   measurements in observing profiles of the Doppler spectrum and the virtual temperature,

336   as shown in the statistics for the comparisons both with radiosonde and with the

337   acoustic speaker RASS. Indeed, the bias and standard deviation for each speaker system

338   RASS with respect to radiosonde were in good agreement with results reported in

21

339   previous studies (e.g., Görsdorf and Lehmann 2000), despite no correction for vertical

340   velocity, which could have been partly because of the experiments being conducted on

341   fine days with light wind and the application of a relatively long averaging time. In

342   addition, removing the first gate data from the statistics may also contribute to the

343   results.

344   Although applying a long averaging time could mitigate the effect of vertical

345   airflow on bias (e.g., Moran and Strauch, 1994), it may degrade the statistics when the

346   virtual temperature profile evolves within the duration of the RASS measurement. On

347   the other hand, the statistics also indicated that the data number associated with the PAA

348   was smaller than that of the acoustic speakers (e.g., Fig. 6), implying that the mean

349   height coverage with the former was lower than that of the latter presumably because of

350   wind in addition to the low peak power mentioned previously. Thus, we independently

351   focus our attention on both the effects of the time evolution of the temperature profile

352   on the statistics and of wind on the height coverage of the RASS measurement in the

353   following sections.

354

4.1 Effect of rapid time evolution of temperature profile

355   **4.1 Effect of rapid time evolution of temperature profile**

356   In the comparisons, the RASS data were averaged for a relatively long time to minimize

357   the effects of both vertical velocity and the spatial difference between the radiosonde

358   and the profiler with RASS. However, the temperature profiles derived from radiosonde

359   observations may not be well suited for use as standard reference data if the temperature

360   profile evolved rapidly within the hour-long RASS observation duration. In the

361   experiments, since the operational radiosondes were launched in the morning of fine

362   days, an inversion layer was frequently observed (Fig. 6) as expected. In fact, 12

363   inversions including multiple inversion layers (e.g., Fig. 6b) were observed in 8 of the

364   16 experiments. Inversion layers can evolve in a relatively short time due to surface

365   heating and cooling and/or the development of the boundary layer in the morning.

366   Indeed, the surface virtual temperature increased by 2.3°C on average with a standard

367   deviation of 1.0°C within an hour for the experiments shown in Fig. 6. Thus, the

368   temperature profile measured with the radiosonde can differ from the mean temperature

369   profile obtained from RASS even though both measurements represented an actual

370   profile, which may result in degrading the statistics for the RASS evaluation.

371   A sample of the temperature profile observing an inversion layer is shown in Fig.

372   8. This observation was made more than 3 h after sunrise (05:15 JST) on that day. The

373   *Tv* profiles with error bars were the mean RASS measurements averaged over an hour

374   from acoustic (red) and PAA (blue) speakers. Both RASS profiles represented the

375   radiosonde profile to some extent but did not follow the profile well, especially around

376   the inversion layer. The large standard deviations indicated by long error bars may

377   reflect the time evolution of the temperature profile in addition to the measurement

378   precision of RASS. By contrast, the 1 min raw RASS data recorded around the

379   radiosonde launch time represented the inversion layer better than the mean RASS

380   measurements at some points, although there were still some discrepancies, which may

381   have been due to the locality of the inversion layer, the effects of vertical air motion or

382   turbulence, or the time difference between RASS and radiosonde in addition to the

383   accuracy and precision of the RASS measurements. The discrepancy above the

384   inversion layer may be caused by the locality of the temperature, because the MRI

385   observation field covered by vegetation (Adachi et al., 2005) ends about 500 m from the

386   profiler, which corresponds to the horizontal displacement at that height. On the other

387   hand, the discrepancies in and below the inversion could be mitigated by considering

388   the effect of the vertical airflow and/or applying a range correction. In terms of the time

389   difference, it is noteworthy that the radiosonde measurement is not a snapshot but

390   sequential; it took more than 2 min for the radiosonde to ascend to an altitude of 800 m

391   AGL, and the temperature profile may evolve even during this time. Thus, a comparison

392   with measurements that have both small spatial difference and high time resolution is

393   needed to evaluate the PAA-RASS measurement.

394

395   **4.2 Comparison with acoustic speaker RASS**

396   To suppress the effects of the spatial and time difference between the two

397   platforms on the evaluation, we next compared the temperatures derived from the

398   PAA-RASS with that from the acoustic speaker RASS. Of course, this comparison does

399   not provide an absolute but relative evaluation of the PAA-RASS measurement. This

400   issue should be kept in mind in examining the intercomparisons presented in this

401   section. In the intercomparison, the requirements for high-quality upper-air reference

402   data (bias $\leq 0.1K$, $\sigma \leq 0.2K$) proposed by WMO (2007) for the GRUAN were used as

403   criteria for the evaluation, although they are not for virtual temperature but for real

404   temperature.

405   A normalized frequency diagram and scatterplot of virtual temperature obtained

406   by the acoustic speaker RASS versus the PAA-RASS are shown in Fig. 9. The 1 min

407   raw data obtained alternately are presented in Fig. 9a, whereas the data averaged for

408   about an hour are plotted in Fig. 9b. Figure 9a shows that the PAA-RASS

409   measurements of virtual temperature were generally in good agreement with those of

410   the acoustic speaker RASS despite disregarding the time difference in the two systems.

411   The linear regression line was close to the one-to-one relation, and the correlation

412   coefficient was close to unity. Moreover, the mean bias and standard deviation of the

413   difference between the two speaker systems were less than 0.1°C and close to 0.4°C,

414   respectively, which are comparable with those obtained by the comparison with

415   radiosonde (Fig. 7) despite the higher time resolution. Since the spatial difference was

416   negligible and the time difference was quite small, the reason for this discrepancy could

417   include temperature fluctuation due to turbulence. Indeed, the mean (max and min)

418   increase of the virtual temperature at the surface for all the experiments was

419   0.2 ± 0.5°C/10 min (1.4°C/10 min, -1.3°C/10 min), which suggests that temperature

420   fluctuation aloft was occurring.

421   A scatter diagram comparing the mean acoustic speaker RASS measurements

422   with those from the parametric speaker RASS is shown in Fig. 9b. The data were

423   averaged over about an hour to minimize the effect of temporal fluctuation of

424   temperature and improve the statistics. Indeed, the linear regression was close to the

425   one-to-one relation, and the correlation coefficient was closer to unity. In addition, both

426   the bias (0.06°C) and standard deviation (0.16°C) improved and satisfied the WMO

427   requirements.

428   From the evaluations mentioned above, we conclude that the accuracy and

429   precision of the parametric speaker RASS are comparable with those of the acoustic

430   speaker RASS for measuring the vertical profile of virtual temperature. The reliability

431   of the parametric speaker RASS could be improved by applying the time average over

432   the appropriate period, advanced quality control, and/or corrections for both range and

433   vertical airflow as long as the effect of the ground clutter is negligibly small.

434

435   **4.3 Effect of horizontal wind on the height coverage of the RASS measurement**

436   The reliability of the parametric speaker RASS measurement was shown to be

437   equivalent to the acoustic speaker RASS. However, we found many instances in which

438   the former tended to have less height coverage than the latter (Figs. 4, 5, and 6), which

439   may also be reflected by the fewer number of data in the statistics (Figs. 6, 7, and 8).

440   Although the parametric speaker system exhibited less peak power than the acoustic

441   speaker system, the weak power cannot be the only reason for the lower height coverage

442   because the results show that the former can observe up to the highest range gate as the

443   latter in some conditions (e.g., Figs. 5a, 5b, 6a, and 8). On the other hand, the results

444   also suggest that the reason may include the effect of wind aloft (e.g., Fig. 5a). Because

445   the acoustic beam generated by the parametric speaker is narrow, it could be susceptible

446   to the horizontal airflow, which displaces the acoustic wave from the radar antenna as

447   shown in Fig. 5. Thus, the effect of horizontal wind on the height coverage of the

448   parametric speaker RASS measurement was evaluated by comparing it with the

449   radiosonde wind data.

450   A scatter diagram comparing the mean RASS height coverage and horizontal

451   displacement of the center of the sound for RASS from that of radio wave at 1200 m

452   AGL is shown in Fig. 10, as well as the mean wind speed aloft. The horizontal

453   displacement was estimated by acoustic ray tracing. In the estimation, the initial

454   displacement of the acoustic speaker system from the profiler antenna on the ground

455   was set at 0 m, because the antenna is surrounded by the four acoustic speakers,

456   whereas that of the PAA was set at 4 m (Fig. 1a). The wind speed aloft is the mean wind

457   from 20 to 1200 m AGL (Table 3), which is the highest mean coverage of the

458   parametric speaker RASS measurements in calm wind conditions (< 2 m s^{-1}) as shown

459   in the figure. The data measured on 30 November 2016 are not considered in the

460   analysis because the RASS measurement was made more than 40 min later than the

461   radiosonde observation (Table 3). Note that the mean RASS height coverage shown in

462   the figure is different from the height coverage of the mean virtual temperature profile

463   in Fig. 6, because the latter reflects the maximum height coverage within the observed

464   profiles after quality control in the duration of the RASS measurement. The long error

465   bars may reflect the large time evolution of the RASS height coverage, which may also

466   be related to the evolution of the wind in the duration.

467   The parametric speaker RASS measurements tended to reach less altitude than the

468   acoustic speaker RASS, even when the horizontal displacement is less than 10 m

469   (corresponding to a wind speed of around 4 m s^{-1}). The reason for the lower coverage

470 under small displacement (light wind) conditions may include the parametric speaker's

471 lower peak power than that of the acoustic speaker system. The height coverage

472 decreased with the displacement and/or wind speed for the parametric speaker RASS, as

473 indicated by the linear regression analysis. In contrast, when the displacement is less

474 than 16 m (corresponding to a wind speed of around 6 m s^{-1}), most of the acoustic

475 speaker RASS measurements achieved a height coverage of around 1300 m AGL,

476 which was the highest range gate for the RASS measurement (Table 1). This suggests

477 that the acoustic speaker RASS keeps on observing at a high altitude even in relatively

478 high wind conditions, as also indicated by the short error bars.

479   It is noteworthy, however, that the height coverage of RASS with acoustic

480 speakers drops sharply to 1000 m AGL at a horizontal displacement of 15–16 m and

481 exhibits a tendency to decrease with the displacement afterward as the parametric

482 speaker RASS. By contrast, the height coverage of the parametric speaker tends to

483 decrease monotonically with the displacement at almost all ranges. These results

484 suggest that the parametric speaker RASS is more sensitive to wind because of the

485 narrow beam, whereas the acoustic speaker RASS is surprisingly robust. Since the four

486 acoustic speakers were not adjusted in phase, this robustness could be explained by the

487 higher aggregate sound power than that shown in Fig. 2 and possible location of sound

488 wave above the antenna in spite of relatively high winds.

489 To compensate for the lower wind tolerance, two additional experiments were

490 performed, in which the acoustic beam was broadened and steered. The parametric

491 speaker system employed for the RASS experiments was equipped with FPGA that

492 controlled the beam pattern of the sound, including beam width and direction. We

493 broadened the beam width from 5° to 12° (Fig. 2) when the parametric RASS echo was

494 observed up to an altitude of 1200 m AGL. However, this experiment resulted in a

495 decrease of the height coverage to 500 m AGL. The height coverage decrease could

496 have been due to the decrease of the peak power associated with beam broadening. In

497 fact, the measured peak power was decreased by 15 dB in our system by broadening the

498 beam (Fig. 2). Therefore, by using this technique, a parametric speaker with more peak

499 power was needed in our case to acquire equivalent height coverage with the acoustic

500 speaker system, which may result in increasing both the size and cost of the system.

31

501   On the other hand, the peak power does not decrease significantly with the zenith

502   angle of the beam as long as the angle is small. The SPL pattern at multiple zenith

503   angles measured in the field is shown in Fig. 11. The peak power was decreased by

504   about 7.5 dB by reducing the power supply to the PAA amplifier, which decreased not

505   only the audible sound but also the ultrasound levels for practical reasons (noisy) and

506   measurement safety. The results indicated that the peak power decreased by only 3.8 dB

507   when the beam was steered to a zenith angle of 10°, which corresponds to a horizontal

508   wind speed of 60 m s^{-1}. The sound wave might be displaced by the horizontal wind but

509   advected to above the antenna if the wave is generated windward with an appropriate

510   zenith angle. Thus, we conducted another experiment with the acoustic beam zenith

511   angle of 2° windward on a day when a mean wind speed of about 12 m s^{-1} between 200

512   and 1200 m AGL was observed with the wind profiler. Unfortunately, no RASS echo

513   was observed, which may be partly because the sound wave did not propagate vertically

514   to the ground, and the advected sound wave front above the antenna was not normal to

515   the propagation direction of the radio wave. Additionally, the acoustic wave front may

516   have been distorted by wind shear. In that case, the radio wave might have been steered

32

517 to the direction normal to the sound wave front by considering the advection and

518 distortion of the sound wave front from the wind profiler measurements.

519

520 **4.4 Health effects of ultrasound exposure**

521 Since the ultrasonic SPL generated by the PAA is extremely high (>200 dB), the health

522 effects of ultrasound exposure in the area close to the PAA should be considered. In

523 studies involving small animals (WHO, 1982), mild biological changes have been

524 reported during prolonged exposure to airborne ultrasound with levels in the range of

525 95–130 dB at frequencies ranging 10–54 kHz, which become more severe with

526 increasing SPL. Thus, the PAA should not be installed on or under the ground level, as

527 it can be easily accessed by animals. Because the PAA for RASS emits sound vertically,

528 animals aloft, including birds and/or insects, can be exposed to the sound beam.

529 However, those animals are capable of avoiding the risk quite easily, because they can

530 perceive the audible sound from the PAA, and the beam width is very narrow. In fact,

531 no animals, including bugs and/or birds, died so far on the PAA after more than 100 h

532 of operation.

533   On the other hand, no adverse physiological or auditory effects appear to occur in

534   humans exposed to sound pressure levels up to about 120 dB (WHO, 1982; Health

535   Canada, 1991). At 140 dB, mild heating may be felt in the skin clefts. With increasing

536   sound pressure levels, the human body becomes warmer until death from hyperthermia

537   has been estimated to occur at levels greater than 180 dB. This lethal threshold value

538   corresponds to a distance of less than 17 m from the PAA, with an ultrasonic SPL of

539   200 dB, assuming an atmospheric attenuation of 1.2 dB m^{-1} (Fig. 3). To avoid

540   ultrasound exposure, we installed the PAA on top of a shed with a height of 2 m so that

541   the speaker won't be accessed by anyone. Moreover, rotational warning lights were

542   installed on the wall of the shed (Fig. 1d) to alert people to the emission of ultrasound

543   more than 50 dB (yellow) and/or 100 dB (red).

544

545   **5 Conclusions**

546   We investigated the applicability of parametric speakers to RASS for measuring

547   the vertical profile of virtual temperature by comparing the data with those obtained

548   from both radiosonde and the acoustic speaker RASS. In the experiments, the

549   operations of the two speaker systems were swapped every minute alternately for the

550 comparison. A detailed analysis of the profiles of both the acoustic attenuation and the

551 Doppler spectrum suggest that although the primary ultrasound generated by the

552 parametric speaker may be dissipated greatly as altitude increases, the secondary

553 audible waves generated from the bifrequency ultrasound can propagate long distances

554 while satisfying the Bragg condition.

555   We have also compared parametric speakers with both radiosonde and acoustic

556 speakers to estimate the reliability of RASS in measuring the virtual temperature (Tv).

557 The results indicated that Tv measured with parametric speaker RASS has comparable

558 reliability with the acoustic speaker RASS measurements; the bias and standard

559 deviation (0.1°C, 0.4°C) for the parametric speaker were close to those for the acoustic

560 speaker (0.0°C, 0.4°C) with respect to radiosonde, which was consistent with the results

561 reported in previous studies, although the conditions in those studies, including the

562 corrections for the vertical wind and/or range, were different from ours. We also found

563 that not only the spatial difference between the two platforms but also both the

564 evolution of the temperature profile during the RASS measurement and temperature

565 fluctuation due to turbulence could contribute to deteriorate the statistics. To mitigate

35

566   these effects, a comparison of virtual temperature obtained from the two speaker

567   systems was also performed. The results indicated that the bias and standard deviation

568   (0.1°C, 0.2°C) of the parametric speaker RASS were quite small and satisfied the

569   requirements for high-quality upper-air reference data proposed by the WMO (2007).

570   Taken together, we conclude that parametric speaker RASS has comparable accuracy

571   and precision with acoustic speaker RASS with respect to the measurement of the

572   virtual temperature profile.

573   We examined the height coverage of RASS and found that the parametric speaker

574   deployed in the experiments tended to have less coverage than the acoustic speakers,

575   which may be a result of the parametric speaker having high directivity, and the

576   generated sound was more susceptible to the displacement from the radar antenna by

577   horizontal wind than the sound wave by the acoustic speakers. Thus, we broadened the

578   beam width of the parametric speaker, which resulted in degrading height coverage

579   because this operation deteriorates the peak power of the audible sound. The sound

580   wave was then steered windward so that the advected sound was located above the

581   antenna. However, no echo was observed, presumably because the sound wave front

582 advected to above the antenna was not normal to the propagation direction of the radio

583 wave in the experiments. In addition, the sound wave front may have been distorted by

584 wind shear. This issue might be solved by using wind profilers that are capable of

585 steering the radio wave (e.g., Adachi and Kobayashi, 2001; Law et al., 2002; Palmer et

586 al., 2005) to the direction normal to the sound wave front as Masuda (1988) proved with

587 the MU radar (Fukao et al., 1985).

588   The results of this study including the statistics do not necessarily apply to all

589 locations, altitudes, and seasons; in particular, we note that the comparisons in this case

590 study were made in the morning on fine days with light wind when the effects of

591 horizontal and vertical wind would be less expected. This condition is possible even in

592 other seasons, but frequency is likely to be less.

593   In summary, we confirm that a parametric speaker is applicable to RASS

594 measurement with a reliability comparable with acoustic speakers. Although it is

595 sensitive to horizontal wind, this type of speaker could be installed to wind profilers

596 located in urban areas for continuous-operational observations (e.g., Ishihara et al.,

597   2006) to improve weather forecast because it has high directivity and no horizontal

598   sound wave leaks to annoy nearby residents.

599

612

613 **Appendix**

614 **Calculation of the atmospheric attenuation**

615 The method of estimating attenuation coefficient for atmospheric absorption from

616 temperature, humidity, and pressure is summarized here based on ISO 9613-1 (ISO,

617 1993). The attenuation coefficient α (dB m^{-1}) is expressed by the sum of four terms in

618 good approximation as

619 $$\alpha = \alpha_{cl} + \alpha_{rot} + \alpha_{vib,O} + \alpha_{vib,N}, \qquad\qquad\qquad (A1)$$

620 where α_{cl} represents the classical absorption caused by the transport processes, α_{rot} is

621 the molecular absorption by rotational relaxation, and $\alpha_{vib,O}$ and $\alpha_{vib,N}$ indicate the

622 molecular absorption caused by vibrational relaxation of oxygen and nitrogen,

623 respectively. The molecular absorption by other compositions of the air including

624 carbon dioxide is small and neglected in the calculation.

625   The first two terms of Eq. (A1) related to the classical and rotational absorption is

626 given by their sum, α_{cr}

627 $$\alpha_{cr} = \alpha_{cl} + \alpha_{rot} = 1.60 \times 10^{-10} \left(\frac{T}{T_0}\right)^{\frac{1}{2}} \left(\frac{P_a}{P_r}\right)^{-1} f^2, \qquad\qquad (A2)$$

628   where T (K) is the atmospheric temperature, T_0 is the reference air temperature (293.15

629   K), P_a (hPa) is the atmospheric pressure, P_r (hPa) is the reference air pressure (1013.25

630   hPa), and f (Hz) is the sound frequency.

631   The two vibrational relaxation terms in Eq. (A1) are given respectively by,

632
$$\alpha_{vib,O} = [(\alpha\lambda)_{max,O}] \times \frac{f}{c_s} \times \left\{ 2\left(\frac{f}{f_{rO}}\right)\left[1 + \left(\frac{f}{f_{rO}}\right)^2\right]^{-1}\right\}, \qquad (A3)$$

633   and

634
$$\alpha_{vib,N} = [(\alpha\lambda)_{max,N}] \times \frac{f}{c_s} \times \left\{ 2\left(\frac{f}{f_{rN}}\right)\left[1 + \left(\frac{f}{f_{rN}}\right)^2\right]^{-1}\right\}, \qquad (A4)$$

635   where subscripts O and N represent oxygen and nitrogen, respectively, $[(\alpha\lambda)_{max}]$ (dB

636   m^{-1}) represents the maximum attenuation by a vibrational relaxation over a distance of a

637   wavelength, λ (m), c_s (m s^{-1}) is the sound speed, and f_r (Hz) is the relaxation frequency.

638   The maximum attenuation by a vibrational relaxation for oxygen and nitrogen are

639   given respectively by,

640
$$[(\alpha\lambda)_{max,O}] = \left(\frac{40\pi}{35}\right)(log_{10}e)X_O\left(\frac{\theta_O}{T}\right)^2 exp\left(-\frac{\theta_O}{T}\right), \qquad (A5)$$

641

642
$$[(\alpha\lambda)_{max,N}] = \left(\frac{40\pi}{35}\right)(log_{10}e)X_N\left(\frac{\theta_N}{T}\right)^2 exp\left(-\frac{\theta_N}{T}\right), \qquad (A6)$$

643   where X_O (= 0.209476) and X_N (=0.78084) represent the standard molar concentrations

644   of dry air, and θ_O (=2239.1 K) and θ_N (=3352.0 K) are the characteristic vibrational

645   temperature for oxygen and nitrogen, respectively.

646   The sound speed c_s in Eq. (A3) and (A4) at a molecular concentration of water

647   vapor of h (%) is given by

648
$$c_s = c_a \times \sqrt{1 - \frac{h}{100}\left(\frac{\gamma_w}{\gamma_a} - \varepsilon\right)} = c_0 \times \sqrt{\frac{T}{T_0}} \times \sqrt{1 - \frac{h}{100}\left(\frac{\gamma_w}{\gamma_a} - \varepsilon\right)} \,, \tag{A7}$$

649   where C_a is the sound speed for dry air, γ_w (=1.33) and γ_a (=1.40) are heat capacity ratio

650   for water vapor and dry air, respectively, ε (=0.662) is the ratio of the molecular weight

651   of water vapor to the molecular weight of air, and C_0 is the sound speed for dry air at

652   the reference air temperature, T_0. The value of h is given from the relative humidity, h_r

653   (%) by

654
$$h = h_r\left(\frac{P_{sat}}{P_r}\right) \Big/ \left(\frac{P_a}{P_r}\right) = h_r\left(\frac{P_{sat}}{P_a}\right) \,, \tag{A8}$$

655   where P_{sat} (hPa) is the saturation vapor pressure given by

656
$$P_{sat} = P_r \times 10^{\left(-6.8346 \times \left(\frac{T_{01}}{T}\right)^{1.261} + 4.6151\right)} \,, \tag{A9}$$

657   and T_{01} (=273.16 K) is the triple-point isotherm temperature. The sound speed in dry air

658   C_a is given by

659 $$c_a = \sqrt{\frac{\gamma_a R}{M_d} T} \ , \qquad\qquad\qquad (A10)$$

660 where R (= 8.314 J mol^{-1} K^{-1}) is the universal gas constant, and M$_d$ (=2.896×10^{-2} kg

661 mol^{-1}) is the molecular weight for dry air. By substituting values of R, and M_d to Eq.

662 (A10), we may derive

663 $$c_a = 20.048\sqrt{T} \ , \qquad\qquad\qquad (A11)$$

664 and $C_0 = 343.25$ m s^{-1} at a temperature of T_0. Note that Eq. (A11) corresponds to Eq. (1)

665 in stationary atmosphere because air temperature T is equal to virtual temperature T_v in

666 dry air.

667   The relaxation frequency for O and N are given by,

668 $$f_{rO} = \left(\frac{P_a}{P_r}\right)\left(24 + 4.04 \times 10^4 h \frac{0.02+h}{0.331+h}\right) \ , \qquad\qquad (A12)$$

669 and

670 $$f_{rN} = \left(\frac{P_a}{P_r}\right)\left(\frac{T}{T_0}\right)^{-\frac{1}{2}} \times \left[9 + 280h + exp\left[-4170\left\{\left(\frac{T}{T_0}\right)^{-\frac{1}{3}} - 1\right\}\right]\right] \ , \qquad (A13)$$

671 respectively.

672   By substituting Eqs. (A2) — (A11) to Eq. (A1), we may derive,

673 $$\alpha \approx 8.686 f^2\left[\left\{1.84 \times 10^{-11}\left(\frac{P_a}{P_r}\right)^{-1}\left(\frac{T}{T_0}\right)^{\frac{1}{2}}\right\} + \left(\frac{T}{T_0}\right)^{-\frac{5}{2}} \times \left\{0.01275 \times\right.\right.$$

674 $$\left.\left. exp\left(\frac{-2239.1}{T}\right)\right\}\left\{f_{rO} + \left(\frac{f^2}{f_{rO}}\right)\right\}^{-1} + 0.1068 \times exp\left(\frac{-3352.0}{T}\right)\left\{f_{rN} + \left(\frac{f^2}{f_{rN}}\right)\right\}^{-1}\right], \ (A14)$$

675   where f_{r0} and f_{rN} are given by Eqs. (A12) and (A13), respectively.

676   The attenuation coefficients at 3 kHz and 40 kHz as a function of temperature and

677   relative humidity estimated using Eq. (A14), is shown in Fig. A1. This figure indicates

678   that the attenuation coefficient for ultrasound at 40 kHz is larger than that for audible

679   sound at 3 kHz, as expected. In addition, the attenuation coefficient depends on the

680   temperature and humidity for both frequencies. Note that the attenuation coefficient for

681   audible sound peaks at lower temperatures (<10°C) than those for ultrasound,

682   suggesting that the attenuation coefficient could increase with altitude for the former,

683   while it decreases for the latter (e.g., Fig. 3, >1 km AGL). In contrast, the contribution

684   of air pressure to the attenuation coefficient on the ground does not differ very much

685   from that at an altitude of 1100 m AGL (~900 hPa).

686 **References**

687 Adachi, A., Clark, W. L., Hartten, L. M., Gage, K. S., and Kobayashi, T.: An
688   observational study of a shallow gravity current triggered by katabatic flow, Ann.
689   Geophys., 22, 3937-3950, doi: 10.5194/angeo-22-3937-2004, 2004.

690 Adachi, A. and Kobayashi, T.: RHI observations of precipitation with boundary wind
691   profiler, Munich, 2001, 116-117.

692 Adachi, A., Kobayashi, T., Gage, K. S., Carter, D. A., Hartten, L. M., Clark, W. L., and
693   Fukuda, M.: Evaluation of three-beam and four-beam profiler wind measurement
694   techniques using a five-beam wind profiler and collocated meteorological tower, J.
695   Atmos. Oceanic Technol., 22, 1167-1180, doi: 10.1175/jtech1777.1, 2005.

696 Adachi, T., Tsuda, T., Masuda, Y., Takami, T., Kato, S., and Fukao, S.: Effects of the
697   acoustic and radar pulse length ratio on the accuracy of radio acoustic sounding
698   system (RASS) temperature measurements with monochromatic acoustic pulses,
699   Radio Sci., 28, 571-583, doi: 10.1029/93RS00359, 1993.

700 Angevine, W. M.: Errors in mean vertical velocities measured by boundary layer wind
701   profilers, J. Atmos. Oceanic Technol., 14, 565-569, doi:
702   10.1175/1520-0426(1997)014<0565:EIMVVM>2.0.CO;2, 1997.

703 Angevine, W. M., Bakwin, P. S., and Davis, K. J.: Wind profiler and RASS
704   measurements compared with measurements from a 450-m-tall tower, J. Atmos.
705   Oceanic Technol., 15, 818-825, doi:
706   10.1175/1520-0426(1998)015<0818:Wparmc>2.0.Co;2, 1998.

707 Angevine, W. M. and Ecklund, W. L.: Errors in radio acoustic sounding of temperature,
708   J. Atmos. Oceanic Technol., 11, 837-842, doi:
709   10.1175/1520-0426(1994)011<0837:EIRASO>2.0.CO;2, 1994.

710 Angevine, W. M., Ecklund, W. L., Carter, D. A., Gage, K. S., and Moran, K. P.:
711   Improved radio acoustic sounding techniques, J. Atmos. Oceanic Technol., 11,
712   42-49, doi: 10.1175/1520-0426(1994)011<0042:IRAST>2.0.CO;2, 1994.

713 Bennett, M. B. and Blackstock, D. T.: Parametric array in air, J. Acoust. Soc. Am., 57,
714   562-568, doi: 10.1121/1.380484, 1975.

715 Berktay, H. O. and Leahy, D. J.: Farfield performance of parametric transmitters, J.
716   Acoust. Soc. Am., 55, 539-546, doi: 10.1121/1.1914533, 1974.

717 Bianco, L. and Wilczak, J. M.: Convective boundary layer depth: Improved
718   measurement by Doppler radar wind profiler using fuzzy logic methods, J. Atmos.

Oceanic Technol., 19, 1745-1758, doi: 10.1175/1520-0426(2002)019<1745:CBLDIM>2.0.CO;2, 2002.

Carter, D. A., Gage, K. S., Ecklund, W. L., Angevine, W. M., Johnston, P. E., Riddle, A. C., Wilson, J., and Williams, C. R.: Developments in UHF lower tropospheric wind profiling at NOAA's Aeronomy Laboratory, Radio Sci., 30, 977-1001, doi: 10.1029/95RS00649, 1995.

Chandrasekhar Sarma, T. V., Narayana Rao, D., Furumoto, J., and Tsuda, T.: Development of radio acoustic sounding system (RASS) with Gadanki MST radar – first results, Ann. Geophys., 26, 2531-2542, doi: 10.5194/angeo-26-2531-2008, 2008.

Ecklund, W. L., Carter, D. A., and Balsley, B. B.: A UHF wind profiler for the boundary layer: Brief description and initial results, J. Atmos. Oceanic Technol., 5, 432-441, doi: 10.1175/1520-0426(1988)005<0432:AUWPFT>2.0.CO;2, 1988.

Fukao, S., Sato, T., Tsuda, T., Kato, S., Wakasugi, K., and Makihira, T.: The MU radar with an active phased array system: 1. Antenna and power amplifiers, Radio Sci., 20, 1155-1168, doi: 10.1029/RS020i006p01155, 1985.

Gan, W.-S., Yang, J., and Kamakura, T.: A review of parametric acoustic array in air, Appl. Acoust., 73, 1211-1219, doi: 10.1016/j.apacoust.2012.04.001, 2012.

Görsdorf, U. and Lehmann, V.: Enhanced accuracy of RASS-measured temperatures due to an improved range correction, J. Atmos. Oceanic Technol., 17, 406-416, doi: 10.1175/1520-0426(2000)017<0406:Eaormt>2.0.Co;2, 2000.

Hashiguchi, H., Fukao, S., Moritani, Y., Wakayama, T., and Watanabe, S.: A lower troposphere radar: 1.3-GHz active phased-array type wind profiler with RASS, J. Meteor. Soc. Japan, 82, 915-931, doi: 10.2151/jmsj.2004.915, 2004.

Health Canada: Guidelines for the safe use of ultrasound: Part II Industrial and commercial applications, Safety Code 24, available online at: http://www.hc-sc.gc.ca/ewh-semt/alt_formats/hecs-sesc/pdf/pubs/radiation/safety-code_24-securite/safety-code_24-securite-eng.pdf, Minister of supply and services Canada, 1991.

Ishihara, M., Kato, Y., Abo, T., Kobayashi, K., and Izumikawa, Y.: Characteristics and performance of the operational wind profiler network of the Japan Meteorological Agency, J. Meteor. Soc. Japan, 84, 1085-1096, doi: 10.2151/jmsj.84.1085, 2006.

751 ISO: 9613-1, Acoustics - Attenuation of sound during propagation outdoors - Part 1:
752   Calculation of the absorption of sound by the atmosphere, ==available online at:==
753   ==https://www.iso.org/standard/17426.html==, 30pp, 1993.

754 ISO: 9613-2, Acoustics - Attenuation of sound during propagation outdoors - Part 2:
755   General method of calculation, 1996. 18pp, 1996.

756 Johnston, P. E., Hartten, L. M., Love, C. H., Carter, D. A., and Gage, K. S.: Range
757   errors in wind profiling caused by strong reflectivity gradients, J. Atmos. Oceanic
758   Technol.,   19,   934-953,   doi:
759   10.1175/1520-0426(2002)019<0934:REIWPC>2.0.CO;2, 2002.

760 Kizu, N., Sugidachi, T., Kobayashi, E., Hoshino, S., Shimizu, K., Maeda, R., and
761   Fujiwara, M.: Technical characteristics and GRUAN data processing for the Meisei
762   RS-11G and iMS-100 radiosondes, GRUAN-TD-5, GRUAN Lead Centre, 2018.

763 Lataitis, R. J.: Signal power for radio acoustic sounding of temperature: The effects of
764   horizontal winds, turbulence, and vertical temperature gradients, Radio Sci., 27,
765   369-385, doi: doi:10.1029/92RS00004, 1992.

766 Law, D. C., McLaughlin, S. A., Post, M. J., Weber, B. L., Welsh, D. C., Wolfe, D. E.,
767   and Merritt, D. A.: An electronically stabilized phased array system for shipborne
768   atmospheric wind profiling, J. Atmos. Oceanic Technol., 19, 924-933, doi:
769   10.1175/1520-0426(2002)019<0924:AESPAS>2.0.CO;2, 2002.

770 Marshall, J. M., Peterson, A. M., and Barnes, A. A.: Combined Radar-Acoustic
771   Sounding System, Applied Optics, 11, 108-112, doi: 10.1364/AO.11.000108, 1972.

772 Martner, B. E., Wuertz, D. B., Stankov, B. B., Strauch, R. G., Westwater, E. R., Gage,
773   K. S., Ecklund, W. L., Martin, C. L., and Dabberdt, W. F.: An evaluation of wind
774   profiler, RASS, and microwave radiometer performance, Bull. Amer. Meteor. Soc.,
775   74, 599-614, doi: 10.1175/1520-0477(1993)074<0599:AEOWPR>2.0.CO;2, 1993.

776 Masuda, Y.: Influence of wind and temperature on the height limit of a radio acoustic
777   sounding system, Radio Sci., 23, 647-654, doi: 10.1029/RS023i004p00647, 1988.

778 Matuura, N., Masuda, Y., Inuki, H., Kato, S., Fukao, S., Sato, T., and Tsuda, T.: Radio
779   acoustic measurement of temperature profile in the troposphere and stratosphere,
780   Nature, 323, 426, doi: 10.1038/323426a0, 1986.

781 May, P. T.: Thermodynamic and vertical velocity structure of two gust fronts observed
782   with a wind profiler/RASS during MCTEX, Mon. Wea. Rev., 127, 1796-1807, doi:
783   10.1175/1520-0493(1999)127<1796:TAVVSO>2.0.CO;2, 1999.

784   May, P. T., Moran, K. P., and Strauch, R. G.: The accuracy of RASS temperature
785   measurements, J. Appl. Meteor, 28, 1329-1335, doi:
786   10.1175/1520-0450(1989)028<1329:Taortm>2.0.Co;2, 1989.

787   May, P. T., Strauch, R. G., and Moran, K. P.: The altitude coverage of temperature
788   measurements using RASS with wind profiler radars, Geophys. Res. Lett., 15,
789   1381-1384, doi: 10.1029/GL015i012p01381, 1988.

790   Moran, K. P. and Strauch, R. G.: The accuracy of RASS temperature measurements
791   corrected for vertical air motion, J. Atmos. Oceanic Technol., 11, 995-1001, doi:
792   10.1175/1520-0426(1994)011<0995:TAORTM>2.0.CO;2, 1994.

793   Moran, K. P., Wuertz, D. B., Strauch, R. G., Abshire, N. L., and Law, D. C.:
794   Temperature sounding with wind profiler radars, J. Atmos. Oceanic Technol., 8,
795   606-608, doi: 10.1175/1520-0426(1991)008<0606:Tswwpr>2.0.Co;2, 1991.

796   Neiman, P. J., May, P. T., and Shapiro, M. A.: Radio acoustic sounding system (RASS)
797   and wind profiler observations of lower- and midtropospheric weather systems,
798   Mon. Wea. Rev., 120, 2298-2313, doi:
799   10.1175/1520-0493(1992)120<2298:RASSAW>2.0.CO;2, 1992.

800   Palmer, R. D., Cheong, B. L., Hoffman, M. W., Frasier, S. J., and López-Dekker, F. J.:
801   Observations of the small-scale variability of precipitation using an imaging radar,
802   J. Atmos. Oceanic Technol., 22, 1122-1137, doi: 10.1175/JTECH1775.1, 2005.

803   Peters, G., Hinzpeter, H., and Baumann, G.: Measurements of heat flux in the
804   atmospheric boundary layer by sodar and RASS: A first attempt, Radio Sci., 20,
805   1555-1564, doi: 10.1029/RS020i006p01555, 1985.

806   Peters, G. and Kirtzel, H. J.: Measurements of Momentum Flux in the Boundary Layer
807   by RASS, J. Atmos. Oceanic Technol., 11, 63-75, doi:
808   10.1175/1520-0426(1994)011<0063:Momfit>2.0.Co;2, 1994.

809   Westervelt, P. J.: Parametric Acoustic Array, J. Acoust. Soc. Am., 35, 535-537, doi:
810   10.1121/1.1918525, 1963.

811   White, A. B., Neiman, P. J., Ralph, F. M., Kingsmill, D. E., and Persson, P. O. G.:
812   Coastal orographic rainfall processes observed by radar during the California
813   Land-Falling Jets Experiment, J. Hydrometeor., 4, 264-282, doi:
814   10.1175/1525-7541(2003)4<264:CORPOB>2.0.CO;2, 2003.

815 WHO: Environmental Health Criteria for ultrasound, available online at:
816   http://www.inchem.org/documents/ehc/ehc/ehc22.htm, Environmental Health
817   Criteria 22, 1982.

818 WMO: GCOS Reference Upper-Air Network (GRUAN): Justification, requirements,
819   siting and instrumentation options, GCOS-112, WMO/TD 1379, 2007.

820 Wu, S., Wu, M., Huang, C., and Yang, J.: FPGA-based implementation of steerable
821   parametric loudspeaker using fractional delay filter, Appl. Acoust., 73, 1271-1281,
822   doi: 10.1016/j.apacoust.2012.04.013, 2012.

823 Wulfmeyer, V., Hardesty, R. M., Turner, D. D., Behrendt, A., Cadeddu, M. P., Di
824   Girolamo, P., Schlüssel, P., Van Baelen, J., and Zus, F.: A review of the remote
825   sensing of lower tropospheric thermodynamic profiles and its indispensable role for
826   the understanding and the simulation of water and energy cycles, Rev. Geophys.,
827   53, 819-895, doi: 10.1002/2014RG000476, 2015.

828

829 **List of Tables**

830 Table 1. Parameters of the wind profiler with RASS.

831 Table 2. Characteristics of the MRI parametric speaker.

832 Table 3. List of the comparison experiments, including date, period, sea level

833 pressure, surface temperature, surface wind speed, and mean wind speed

834 aloft (20 – 1200 m AGL).

835

836 **List of Figures**

837 Figure 1. Pictures of (a) LAP-3000 with acoustic speakers and a parametric speaker for

838 RASS, (b) top view, (c) partial expanded view of the parametric speaker, and (d) rotary

839 warning lights on the shed wall. The parametric speaker mounted on top of the shed

840 with a sliding roof is covered with rainproof film in the field, as shown in (a).

841

842 Figure 2. Audible sound pressure level (SPL) pattern for an acoustic speaker (red), the

843 parametric speaker with the measured beam width of 5° (blue) and 12° (black) at a

844 frequency of 3 kHz. The error bars represent 2σ. The SPL pattern for the acoustic

845 speaker in the negative zenith angle region is a mirror image of the pattern measured at

846   the positive zenith angle for ease of viewing. The background noise level was about 50

847   dB. The SPL was measured with a sound level meter (Rion NL-42).

848

849   Figure 3. Profiles of atmospheric-attenuation coefficient α and atmospheric attenuation

850   for sound at frequencies of (a) 3 kHz and (b) 40 kHz derived from the radiosonde

851   measurements at 08:30 JST on 19 October 2016, at the MRI site.

852

853   Figure 4. Doppler spectra from RASS observations measured with (a) acoustic speakers

854   from 08:30 JST for 1 min and (b) the parametric speaker from 08:31 JST for 1 min on

855   19 October 2016. At each height, the first moment of the spectrum, indicated by the

856   vertical bar, gives the vertical sound velocity, and the second moment, indicated by the

857   horizontal bar, gives the spectral width.

858

859   Figure 5. Profiles of received mean RASS echo power, horizontal displacement of the

860   parametric speaker sound from radio wave, and wind speed on (a) 19 October 2016, (b)

861   27 October 2016, (c) 9 August 2017, and (d) 7 September 2017, derived with the

862   acoustic speakers (red), the parametric speaker (blue), and radiosonde (green). The error

863   bars represent 2σ. The black lines indicate linear regressions for the received power data

864   (except for the first range) as shown in the upper-right legend with correlation

865   coefficients.

866

867   Figure 6. Profiles of virtual temperature (Tv) and received power (Pr) from 08:30 JST

868   on (a) 15 October, (b) 21 October, (c) 8 November, and (d) 30 November 2016 derived

869   from a radiosonde (black), RASS with acoustic speakers (red and orange), and the

870   parametric speaker (blue). The radiosonde data were smoothed by 100 m running means

871   to match with the vertical resolution of the RASS. The error bars represent 2σ in the

872   RASS hourly observations. The mean, standard deviation, and number of samples of

873   temperature difference are summarized in a table in each panel.

874

875   Figure 7. Scatterplots of virtual temperature of the RASS vs. the radiosonde

876   measurements at all heights except for the first range. The data derived from the RASS

877   with the acoustic speakers (the parametric speaker) are plotted as open (closed) circles.

878   The radiosonde data were smoothed by 100 m running means to match with the vertical

879   resolution of RASS. The lines represent linear regressions for each data set as shown in

880   an upper legend along with the correlation coefficients. The mean, standard deviation

881   and number of samples of temperature difference are summarized in a bottom table.

882

883   Figure 8. Profiles of the virtual temperature (Tv) from 08:30 JST on 7 September 2017,

884   derived from a radiosonde (black), RASS with acoustic speakers (red), with the

885   parameter speaker (blue), and horizontal displacement of the radiosonde from the

886   profiler (green). The radiosonde data were smoothed by 100 m running means to match

887   with the vertical resolution of RASS. The error bars represent 2σ in the RASS

888   observations averaged over 60 min, and closed circles represent 1 min raw data from the

889   time indicated. The mean, standard deviation, and number of samples of temperature

890   difference of RASS from radiosonde are summarized in the table.

891

892   Figure 9. Comparisons of the parametric speaker vs. the acoustic speakers in measuring

893   virtual temperature at all heights (except for the first gate) shown by (a) a normalized

894   frequency diagram (color scale) and (b) a scatterplot. The data obtained from each

895   speaker system every 1 min alternately were used in (a), whereas the hourly-mean data

896   were plotted in (b). The mean Tv derived with the acoustic speakers is shifted 10°C for

897   ease of viewing in (b). The lines represent linear regressions for each data set, shown in

898   the upper-left and lower-right legends along with correlation coefficients, respectively.

899   The mean, standard deviation, and number of samples of temperature difference are

900   summarized in each table.

901

902   Figure 10. Scatterplots of mean height coverage of RASS measurement vs. horizontal

903   displacement of the beam center of the sound for RASS from that of the radio wave at

904   1200 m AGL derived from radiosonde observations. Closed circles (squares) denote the

905   observed mean RASS height coverage by acoustic speakers (parametric speaker) with

906   standard deviations indicated by error bars. The color scale represents the mean wind

907   speed aloft (20–1200 m AGL). Thick lines represent linear regressions for each data set,

908   where the PAA data are divided by a height threshold of 1100 m AGL. The highest

909   range gate sampled for the RASS measurement is 1300 m AGL.

910

911   Figure 11. ==Audible== sound pressure pattern of the parametric speaker at a frequency of 3

912   kHz measured at multiple zenith angles, shown in the upper legend with the beam width

913   observed. ==Note that the peak SPL was decreased by about 7.5 dB for safety.== The SPL

914   was measured with a sound level meter (Rion NL-42).

915

916   ==Figure A1. Simulated atmospheric-attenuation coefficients for sound at the frequencies==

917   ==of (a) 3 kHz and (b) 40 kHz as a function of the atmospheric temperature and the==

918   ==relative humidity at an atmospheric pressure of 1013 hPa. Results for a pressure of 900==

919   ==hPa are also plotted for a relative humidity of 20%.==